TECHNICAL MEMORANDUM
Conceptual Site Model

Movement of TCE in the Chatsworth Formation

Santa Susana Field Laboratory
Ventura County, California

April 2000

Prepared for
The Boeing Company
Rocketdyne Propulsion and Power Division

Prepared by:
Montgomery Watson
1340 Treat Blvd., Suite 300
Walnut Creek, CA 94596

Richard G. Andrachek, P.E.

J. Ross Wagner, PhD., R.G.

REGISTERED GEOLOGIST
JESSE R. WAGNER
#4312
STATE OF CALIFORNIA

HDMSe00012888

Contents

Volume I

1.0 Introduction 1-1
- 1.1 Facility Description and History 1-1
- 1.2 Problem Overview and Solution Approach 1-2
- 1.3 Information Sources Used to Develop the Conceptual Model 1-3

2.0 Overview of Conceptual Site Model 2-1

3.0 Geology 3-1
- 3.1 Regional Geologic Setting 3-1
- 3.2 Depositional Environment 3-1
- 3.3 Stratigraphy 3-2
- 3.4 Structures 3-3
- 3.5 Preliminary Assessment of Geologic Features on Groundwater Flow 3-4

4.0 Hydrogeology 4-1
- 4.1 Historical Summary 4-1
- 4.2 Estimate of Site Bulk Hydraulic Conductivity from Water Balance 4-1
- 4.3 Hydraulic Conductivity Testing 4-2
- 4.4 Vadose Zone Water Content 4-2
- 4.5 Influence of Stratigraphy and Geologic Structure on Hydraulic Conductivity 4-3
- 4.6 Delineation of Groundwater Units 4-4
- 4.7 Interconnected Nature of Chatsworth Formation Fracture Network 4-5
- 4.8 Groundwater Units 4-5
- 4.9 Hydraulic Apertures, Fracture Porosity and Average Linear Groundwater Velocity 4-6
- 4.10 Summary of Hydrogeology at the SSFL 4-7

5.0 TCE Occurrence at the SSFL 5-1
- 5.1 TCE Input Locations 5-1
- 5.2 Historical and Preliminary RFI Finding 5-1
- 5.3 TCE in Chatsworth Formation Groundwater 5-2

6.0 Flow, Distribution and Fate of TCE DNAPL in Source Zones 6-1
6.1 DNAPL Flow and Distribution in the Vadose Zone 6-2
6.2 Mass Transfer of TCE Between Vadose and Groundwater Zones 6-3
6.3 DNAPL Flow and Distribution in the Saturated Zone 6-3
6.4 Effects of Matrix Diffusion on TCE DNAPL Below the Water Table 6-6
6.5 Summary of Flow, Distribution and Fate of TCE DNAPL In Source Zones 6-8

7.0 Transport and Fate of TCE Solute 7-1
7.1 TCE Solute Transport and Retardation in a Single Fracture 7-2
7.2 TCE Solute Transport and Retardation in a Two Dimensional Fracture Network 7-4
7.3 Comparison of Model Result with Field Data 7-5
7.4 Summary 7-7

8.0 Monitoring Chatsworth Formation Groundwater 8-1
8.1 Interconnected Fracture Network 8-1
8.2 Plume Retardation 8-1
8.3 Dispersion 8-2
8.4 Temporal and Spatial Monitoring 8-3

9.0 Summary of Conceptual Site Model 9-1
10.0 References 10-1

Appendices

Volume II

A. Geologic Characterization
B. Hydrogeology
C. Fracture Aperture Determinations from Bore Hole Information

Volume III

D. Flow and Fate of TCE DNAPL in Vadose Zone and Flow of DNAPL in Saturated Zone
E. Evolution of TCE Source Zones and Plumes in the Chatsworth Formation
F. Modeling Simulations of TCE Solute Transport and Fate in the Chatsworth Formation Groundwater
G. Groundwater Monitoring in Fractured Sandstone and Implications for the SSFL

TECHNICAL MEMORANDUM

Conceptual Site Model

Movement of TCE in the Chatsworth Formation

Santa Susana Field Laboratory, The Boeing Company

1.0 Introduction

This Technical Memorandum presents a conceptual site model[1] of the movement of trichloroethene (TCE) in the Chatsworth Formation at The Boeing Company's (Boeing) Santa Susana Field Laboratory (SSFL). The SSFL is located in the Simi Hills of Ventura County between the Simi and San Fernando Valleys and occupies approximately 2850 acres (Figure 1.1). Previous subsurface environmental investigations have shown the groundwater beneath the SSFL to be impacted by volatile organic compounds (VOCs), with TCE being the compound detected in Chatsworth Formation groundwater at the highest concentration and with the most frequency. Other chemicals are also present within Chatsworth Formation groundwater but at concentrations typically orders of magnitude lower than TCE. The Chatsworth Formation consists mainly of fractured sandstone and is the geologic unit that is present beneath most areas of the SSFL.

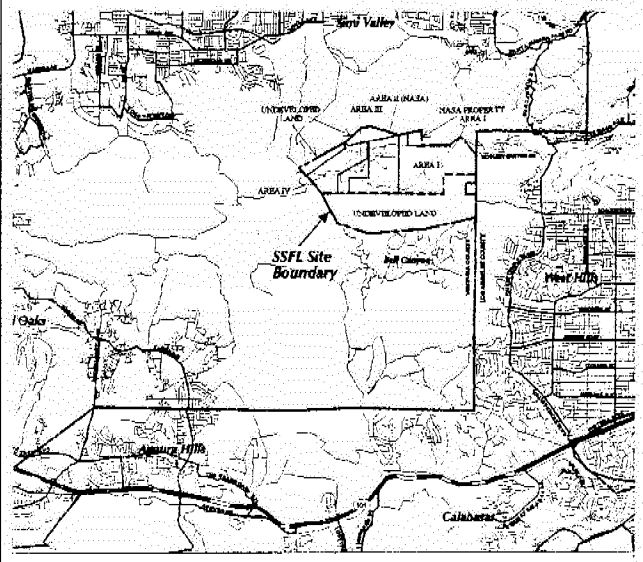

Figure 1.1 SSFL Site Location

[1] A definition of a conceptual site model of environmentally impacted sites is provided by EPA and summarized here. The conceptual site model, like any theory or hypothesis, is a dynamic tool that should be tested and refined throughout the life of the project. The conceptual site model typically is presented as a summary or specific component of a site investigation report. The model is based on, and should be supported by, interpretive graphics, reduced and analyzed data, subsurface investigations, logs and other pertinent characterization information. The conceptual site model is not a mathematical or computer model, although these may be used to assist in developing and testing the validity of a conceptual model or evaluating the restoration potential of the site (EPA 1993).

The conceptual site model discussed in this technical memorandum presents the understanding of the flow, distribution and fate of TCE in unsaturated and saturated portions of the Chatsworth Formation as an immiscible dense non-aqueous phase liquid (DNAPL) and as a solute that is transported by groundwater through the fractured sandstone. The body of this technical memorandum provides a summary of the geologic and hydrogeologic setting, release locations at the SSFL and the primary conclusions on the movement of TCE in the Chatsworth Formation. Documentation and analyses supporting these conclusions are included as appendices.

The conceptual site model was developed by Dr. John Cherry and Dr. Beth Parker from the University of Waterloo, Dr. Dave McWhorter from Colorado State University, (herein after referred to as the Expert Panel), Montgomery Watson, and Haley and Aldrich.

1.1 Facility Description and History

The SSFL is subdivided into five administrative areas: Area I, Area II, Area III, Area IV and undeveloped land (Figure 1.2). Areas I and III and undeveloped land are owned and operated by The Boeing Company, Rocketdyne Propulsion & Power (Rocketdyne). Area II is owned by the U.S. National Aeronautics and Space Administration (NASA) and operated by Rocketdyne. Area IV is owned and operated by Rocketdyne, but includes facilities owned by the U.S. Department of Energy (DOE), which are currently undergoing decommissioning and demolition. Operations conducted in each of these areas have resulted in the Chatsworth Formation groundwater being impacted with TCE.

The SSFL has been operated as a rocket engine testing facility since 1948. Six major rocket engine test areas, including Bowl, Canyon, Alfa, Bravo, Coca, and Delta, were in operation simultaneously in the late 1950's and early 1960's.

HDMSe00012891

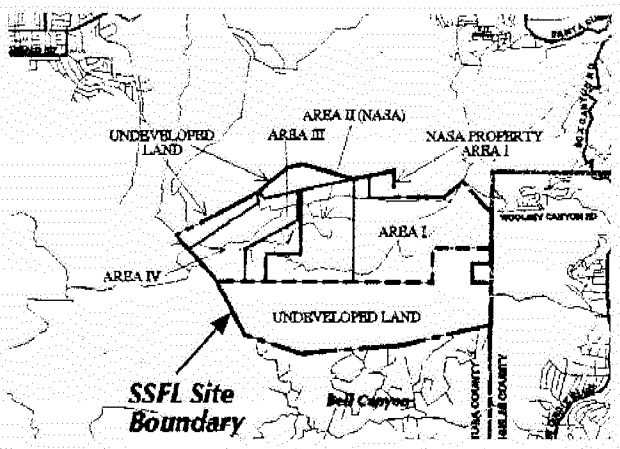

Figure 1.2 Five Administrative Areas at the SSFL

Some of these test areas were phased out of operation in the late 1960's and 1970's. The Coca area was shut down in May 1988. Experimental, small-scale rocket engine testing has taken place at the area now designated APTF. The Alfa, Bravo, and APTF test areas are currently in operation.

Rocketdyne and its predecessor organizations conducted programs for the U.S. Department of Energy (formerly the Atomic Energy Commission and Energy Research and Development Agency) from the early 1950's until 1989 in Area IV. Those programs included engineering, research and development, and manufacturing functions primarily concerned with nuclear reactor development and applications. During the period from 1950 through 1973, Rocketdyne conducted research and development on nuclear reactor subsystems. In 1966, the Energy Technology Engineering Center (ETEC), staffed and operated by Rocketdyne, was chartered by DOE to provide engineering development and testing of components for the Liquid Metal Fast Breeder Reactor Program. ETEC primarily conducted programs for DOE and, with DOE's approval, for other organizations (DOE, 1989). ETEC operations ceased in 1989. Currently in Area IV, Rocketdyne is conducting environmental restoration programs for DOE.

1.2 Problem Overview and Solution Approach

Visual inspections of rock outcrops present throughout the SSFL reveal systematic cracks (fractures or partings) that have large openings (Photograph 1.1). These observations suggest to the casual observer that water flowing onto the ground (precipitation or artificial discharge) would rapidly flow into the subsurface and away from the site through these apparently large fractures. Furthermore, a hydrogeologic analysis of the average linear groundwater velocity in a generic sandstone using Darcy's Law suggests rapid groundwater flow in the range of miles per year or miles per decade (Figure 1.3).

Photograph 1.1 Example of Fractures Exposed in Outcrop at the SSFL

A similar conclusion might also be reached regarding the potential for rapid transport of historical releases of TCE. However, the presence of dissolved TCE in Chatsworth Formation groundwater, observed over the last 15 years, suggests TCE plume fronts have migrated only hundreds to a few thousands of feet from their release locations (Groundwater Resources Consultants, 1999). It is this apparent paradox of rapid groundwater flow coupled with relatively slow transport of TCE plume fronts through the fractured Chatsworth Formation sandstone that is resolved in this technical memorandum through the presentation of the conceptual site model.

AVERAGE LINEAR GROUNDWATER VELOCITY
Sandstone

$$\bar{V} = \frac{K_b\,(dh/dL)}{\phi_f}$$

K_b	10^{-4} cm/s
dh/dL	0.01
ϕ_f	0.001

$\bar{V}$ = 1000 feet per year

Figure 1.3

HDMSe00012892

The approach taken to develop the conceptual model of TCE movement and fate in the Chatsworth Formation involved the following activities:

- The Expert Panel developed an initial conceptual model that attributed the retardation of TCE primarily to molecular diffusion into the sandstone matrix blocks between the fractures (matrix diffusion).
- New field data were collected from near two former TCE source locations to validate this initial model.
- Additional geologic analysis was conducted on the stratigraphy and structure of the Chatsworth Formation and on groundwater flow in the presence of the stratigraphic and structural features.
- All available geologic and hydrogeologic data collected at the SSFL were evaluated to determine whether the initial conceptual site model could be consistently applied throughout the site.
- The TCE retardation-through-matrix diffusion model was evaluated by simulating hydrogeologic conditions through a numerical model of TCE transport in a two-dimensional fracture network using site-specific values for input parameters.

1.3 Information Sources Used to Develop the Conceptual Model

Historic and new information were used to validate the conceptual site model. Historic information dates back to 1948 when the facility first became operational. The sources and types of information used include:

- Documentation provided by Boeing on water supply well operations, water needs and water level changes from the late 1940s to the early 1960s.
- Geologic literature, reports and maps that are available in the public domain.
- Historical data on site hydrogeology and TCE concentrations based on work performed mainly by Groundwater Resources Consultants since the mid-1980s.
- Hydrogeologic and contaminant transport research papers and publications.
- Additional site-specific data that were collected. These data include:

✓ rock matrix porosity, moisture content and permeability measurements,

✓ organic carbon content,

✓ chloride diffusion coefficients,

✓ dry and wet bulk densities,

✓ sampling and analysis of rock pore water for volatile organic compounds (VOCs),

✓ advanced downhole geophysical methods,

✓ joint (or fracture) frequency and orientation,

✓ discrete interval groundwater monitoring systems for hydraulic head and TCE concentrations and,

✓ hydraulic tests using double packers to evaluate the vertical variability in hydraulic conductivity.

HDMSe00012893

2.0 Overview of Conceptual Site Model

As mentioned in section 1.2, observations of the short distances that TCE has migrated from the input locations at the SSFL (hundreds to a few thousands of feet over decades) indicate a strong retardation effect compared to the average linear groundwater velocity (miles per year or decade). The conceptual site model of the movement of TCE in the Chatsworth Formation includes the following three key elements:

1. *TCE DNAPL that was present within the fracture system below the water table dissolves from the fracture due to diffusion into the sandstone matrix.* This element of the conceptual site model was based on earlier work that members of the Expert Panel had conducted regarding molecular diffusion of immiscible-phase organic liquids in fractured geologic media (Parker, Gillham and Cherry, 1994; Parker, McWhorter and Cherry, 1997).

2. *The migration of TCE, once dissolved in groundwater, is retarded relative to the average linear groundwater velocity due to diffusion into and sorption onto the sandstone matrix.* Foster (1975) initially documented the effects of matrix diffusion on the migration of a solute in fractured porous rock. Freeze and Cherry (1979) initially extended this work to include the concept of retardation of a solute plume front.

3. *Matrix diffusion attenuates (or reduces) the dissolved concentrations of TCE in groundwater at the source and in the plume over time.* This effect of matrix diffusion has been conceptualized and demonstrated by work performed by Parker and Cherry directly as a result of this project and is being documented for the first time in this technical memorandum.

Properties that most directly effect diffusion of TCE either as a DNAPL or solute, into the sandstone matrix include:

- matrix porosity,
- aqueous concentration gradients,
- diffusion coefficient,
- fraction of organic carbon , and
- time of diffusion, which is directly linked to fracture aperture and surface area.

Table 2.1 summarizes values of these parameters at the SSFL.

Property	No. of Measurement	Minimum	Maximum	Mean
Porosity (%)	59	1.0	21.60	12.86
Diffusion Coefficient (cm^2/sec)	10	7.5×10^{-7}	2.2×10^{-6}	1.5×10^{-6}
Fraction Organic Carbon (%)	8	0.02	0.15	0.10
Hydraulic Fracture Apertures (microns)	Not applicable [1]	10	300	100

Note: TCE Solubility = 1420 milligrams per liter **Table 2.1**
[1] Calculated using the Cubic Law (Snow, 1968)

The geometry of the fracture system at the SSFL has the greatest uncertainty, and can most significantly affect the initial conceptual model. Therefore, considerable effort was put forth in determining values of the bulk hydraulic conductivity representing various spatial scales ranging from local to site-wide. These hydraulic conductivity values were used to calculate hydraulic apertures at locations where the number of fractures can be reasonably determined. All site data and work performed by the team indicates that the initial model of strong attenuation of the TCE within the sandstone matrix is valid and applicable throughout the site. This conclusion is based on the following elements:

1. *The fractures at the SSFL are small, systematic and interconnected.*

- Calculations of the hydraulic fracture apertures were made using site values for hydraulic conductivity and fracture spacing. Hydraulic apertures ranged between 10 and 300 micrometers (or microns), with a mean value of about 100 microns. For comparison, the diameter of a human hair is about 20 microns.

- Frequent and systematic fractures are present as evidenced by inspections of outcrops and rock core, downhole geophysics tests and the distribution of TCE in rock pore water adjacent to fractures.

HDMSe00012894

- Fracture systems are interconnected as evidenced by pumping test analyses, a hydraulic communication study, groundwater elevation correlations and the presence of TCE in rock pore water at numerous depths throughout the vertical profile of two test boreholes.

- Analysis of pumping test data indicated the absence of high hydraulic conductivity zones along lineaments suggesting that extensive open fractures do not exist.

2. *The small, systematic and interconnected fractures, coupled with the porous sandstone matrix, facilitates diffusion of TCE into the matrix.*

- The conceptual model explaining the general attenuation and retardation of solutes in fractured porous rock, based on Fick's Law of molecular diffusion applied to the rock matrix was first documented by Foster (1975).

- Conceptual models of DNAPL disappearance through diffusion in fractured porous media were put forth by certain members of the Expert Panel in 1994 (Parker, Gillham and Cherry, 1994). Recent field experiments by Kirkpatrick (1998) and laboratory experiments by O'Hara, Parker, Cherry and Jorgensen (2000) have validated this conceptual model.

- The mass storage capacity provided by the porosity of the sandstone matrix for dissolved and sorbed TCE at the SSFL ranges between 5 and 100 times greater than the mass storage capacity of the fracture network to hold DNAPL, indicating that dissolution of TCE DNAPL through matrix diffusion is feasible. Calculations using site-specific data indicate that TCE as a DNAPL is present for periods ranging from 2 to 50 years.

- Diffusion into the sandstone matrix at the SSFL has been documented by chemical analysis of 277 samples of rock core for VOCs (Sterling 1999). Samples were collected from two boreholes placed near TCE input locations. All TCE concentrations detected in rock porewater were less than 10% of the aqueous solubility limit for TCE indicating no DNAPL is present in fractures below the water table.

3. *TCE plume fronts are strongly retarded due to matrix diffusion and the presence of organic carbon, and advance at rates that are orders-of-magnitude slower than the average linear groundwater velocity.*

- The presence of organic carbon within the matrix increases the diffusive mass flux from the fracture to the matrix and retards the migration of TCE by a factor of three.

- Inspection of 15 years of groundwater chemistry data shows that TCE has not migrated far from the input locations.

- Numerical modeling simulations for TCE migration through fracture networks using properties representative of the conditions at the SSFL predict strong retardation of the TCE plume front as it migrates downgradient from the input location and predict the overall decline in concentrations throughout the source zones and plume.

Each of these elements is more fully discussed in the subsequent sections (and appendices) of this technical memorandum.

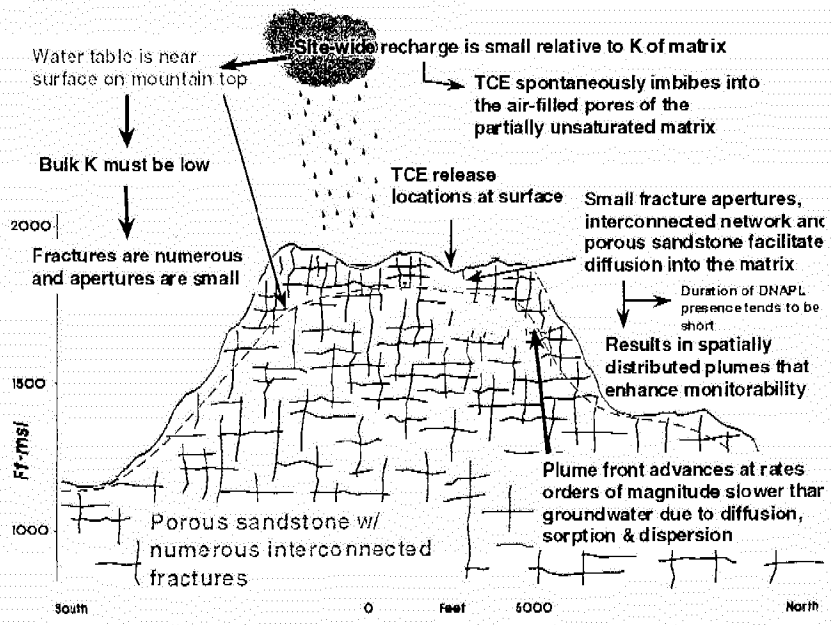

Figure 2.1
Graphic Depiction of Conceptual Site Model

HDMSe00012895

This section of the technical memorandum presents a summary of the geologic framework of the SSFL and focuses on geologic features that have potential implications on groundwater flow. The relationship of these features to groundwater flow will be more fully discussed in Section 4.0. The regional geologic setting, depositional environment, stratigraphy and structures are presented in this section. A more detailed description of the site geology is provided in Appendix A.

3.1 Regional Geologic Setting

SSFL is located in the Transverse Ranges of Southern California, a geologic province that is in north-south compression and in which geologic structures, such as faults and folds, strike in an approximately east-west direction. Most of the site is underlain by late Cretaceous marine turbidites of the Chatsworth Formation (Link, Squires and Colburn, 1981; Dibblee, 1992) (Figure 3.1). The Chatsworth Formation is faulted against the Paleocene Santa Susana Formation in the western part of the site, while in the northern part of the site the Simi Conglomerate Member of the Santa Susana Formation lies in depositional contact on the Chatsworth.

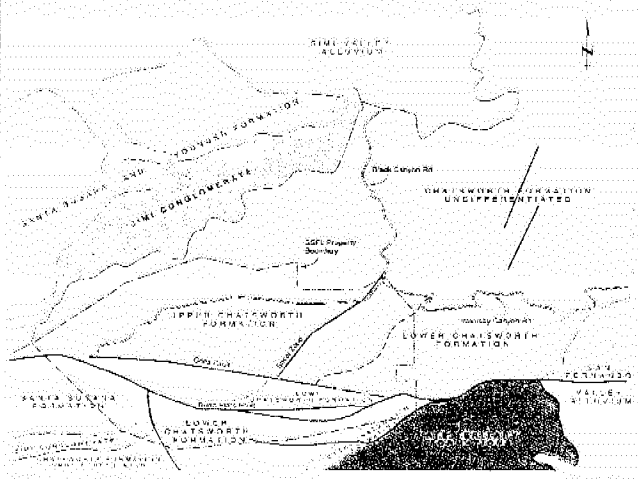

Figure 3.1 **Regional Geologic Setting**

Structurally, the facility is located on the south flank of an east-west striking and westward plunging syncline which passes through the central part of Simi Valley. Bedding at the site typically strikes approximately N70E and dips 25 to 35 degrees to the northwest.

3.2 Depositional Environment

The physical and hydrogeologic characteristics of the Chatsworth Formation are strongly influenced by the depositional environment. Link, Squires, and Colburn (1981) provide the most recent and detailed evaluation of the depositional environment of the Chatsworth Formation and most of this discussion is based on their work.

The Chatsworth Formation is composed primarily of medium-grained sandstone that has been deposited by turbidity currents at a depth of between 600 and 3,000 feet on the middle part of a submarine fan. Figure 3.2 below provides a diagrammatic representation of both the topographic setting and the variation of lithology of a typical submarine fan.

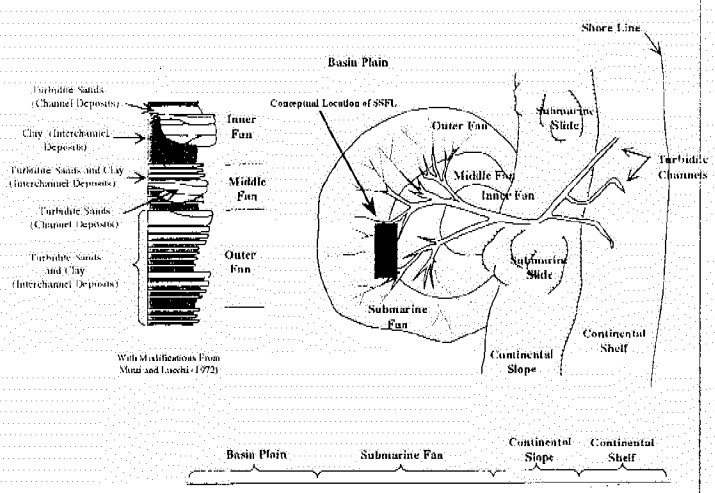

Figure 3.2 **Diagrammatic Map of Submarine Fan**

The fan that created the Chatsworth Formation is interpreted to be highly inefficient because it has a high ratio of sand to shale. The sandstones were deposited as lenticular sand bodies that are locally more than 300 feet thick and 3,000 feet wide. Work completed by Montgomery Watson suggests that parts of the Chatsworth Formation located to the east and south of the operational areas of the SSFL were probably deposited in either an outer fan environment or in the transition zone between the middle and outer fan. These outer fan/transition deposits are characterized by a much

HDMSe00012896

higher proportion of siltstones and shales than found in the middle fan environment.

The finer-grained parts of the Chatsworth Formation are typically composed of a combination of clay shale, siltstone, and lesser amounts of fine-grained sandstone. For ease of discussion, these composite finer-grained units will be referred to as shales.

3.3 Stratigraphy

The Chatsworth Formation at the SSFL has been divided into stratigraphically lower and upper units. The different geomorphic expressions of the upper and lower Chatsworth Formation are shown in Photograph 3.1. The lower Chatsworth Formation is located in the eastern and southern parts of the SSFL and is differentiated from the upper Chatsworth by a much higher proportion of fine-grained material. Approximately half of the upper 1000 feet of the lower Chatsworth stratigraphy is composed of siltstone and mudstone. Most of the sandstones in the lower Chatsworth are fine-grained, with beds typically being less than 3 feet thick.

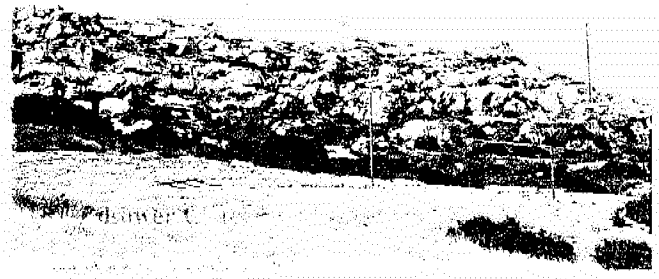

Photograph 3.1 Geomorphic Expression of Lower and Upper Chatsworth Formation

In contrast to the lower Chatsworth, the upper Chatsworth is composed almost exclusively of medium- to fine-grained sandstone. Shale beds are present, but are typically thin and discontinuous. Sandstone beds in the upper Chatsworth are normally less than 30 feet thick and have been deposited directly upon one another. These amalgamated sandstone beds locally reach thicknesses of approximately 200 feet. The sandstones typically show graded and convolute bedding, pebbly basal units, rip-up clasts, and both flute and groove casts.

The upper Chatsworth Formation has been divided into several different hydrostratigraphic units by the presence of two, relatively thin, laterally continuous shale beds called Shale 2 and Shale 3, which were identified during field mapping and confirmed through the review of available literature. A stratigraphic column is shown in Figure 3.3. These units are described below in stratigraphic sequence from oldest to youngest.

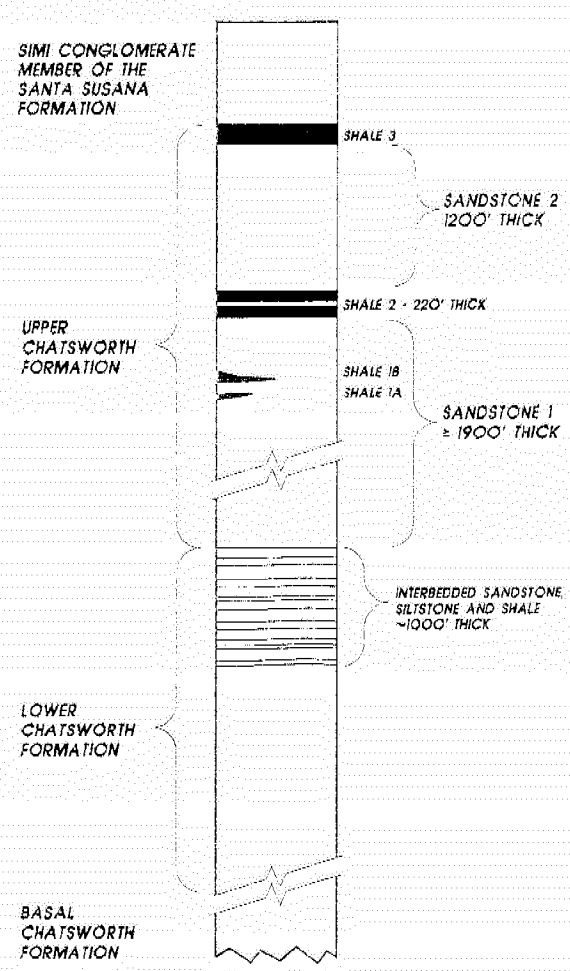

Figure 3.3 Stratigraphic Column

- **Sandstone 1:** Sandstone 1 is defined as the predominantly sandstone section between the top of the lower Chatsworth Formation and the bottom of Shale 2. Sandstone 1 contains a relatively thin shale unit, called Shale 1, which is located in the central part of the SSFL, just south of the Alpha and Bravo test stands. Sandstone 1 also contains at least two other shale units. The Happy Valley Shale is located just east of the Shear Zone, and its northeastward extent has not been

HDMSe00012897

evaluated. A second, relatively thin, shale may be present in the area between the Coca and Burro Flats Faults. This shale is inferred from aerial photos and boring logs, but has not been observed in outcrop.

- **Shale 2:** Shale 2 is located in the middle of the upper Chatsworth and consists primarily of shale and siltstones with beds that are typically less than a foot thick and interbedded with fine-grained sandstones. The shales typically show closely spaced fractures in outcrop.

- **Sandstone 2:** Sandstone 2 is defined as the predominantly sandstone unit which lies between the top of Shale 2 and the bottom of Shale 3. The sandstones of this unit are lithologically very similar to those of Sandstone 1. Sandstone 2 differs from Sandstone 1 both by having very few outcrops in the western part of the SSFL, and by having more widely-spaced joints. Data from both outcrops and boring logs indicate that Sandstone 2 contains a number of relatively thin shale units.

- **Shale 3:** Shale 3 is the stratigraphically uppermost unit in the Chatsworth Formation and its composition is very similar to Shale 2

3.4 Structures

A number of faults are present at the SSFL as shown on Figure 3.4 and generally strike in two directions. One set of faults strikes a northeasterly direction and includes the Shear Zone and the Skyline Fault, while the second set strikes approximately east-west and includes the Burro Flats, Coca, Tank, Happy Valley and North Faults. Locations of all of the faults are shown on Figure 3.4. All of these faults appear to dip nearly vertical based on their exposures. A brief description of each of these faults and other features that may influence groundwater flow is provided below.

- **North Fault:** Long, continuous lineaments observed on aerial photos suggest that the eastern part of the North Fault is probably a relatively continuous feature. Gouge was thin or absent in the existing exposures of the North Fault, and no significant fracturing was observed adjacent to exposed fault traces.

- **Happy Valley Fault:** The Happy Valley Fault creates a strong aerial photo lineament suggesting that the fault is a relatively continuous feature. Fault gouge observed in outcrops of the Happy Valley Fault consists of sandy silt, which ranges from less than 1 inch to approximately 18 inches thick. No significant fracturing was observed in rocks adjacent to the Happy Valley Fault.

- **Tank Fault:** Exposures of the Tank Fault suggest that it is composed of a series of discontinuous failure surfaces that are separated from one another by distances ranging from feet to inches. The exposures also show little or no gouge along the failure surfaces, and an absence of fracturing adjacent to the fault.

Figure 3.4 Geologic Site Map of the SSFL

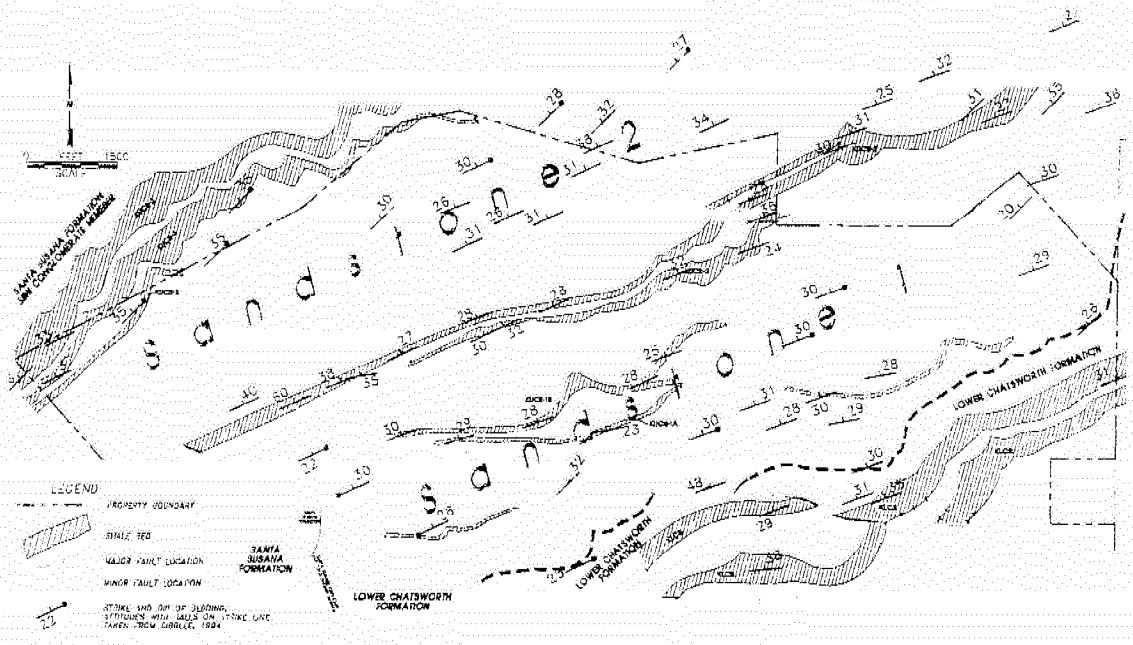

HDMSe00012898

- **Coca Fault:** Well-developed aerial photo lineaments suggest that the Coca Fault is likely composed of relatively long and connected failure surfaces. Exposures in the failure surfaces of the Coca Fault suggest there is modest gouge development along some of them. Up to 4 inches of gouge was observed on one failure surface, but gouge was absent on a second exposed failure surface. There is little or no fracturing adjacent to exposed failure surfaces of the Coca Fault.

- **Burro Flats Fault:** The Burro Flats Fault creates a very continuous and well-developed, linear topographic low in the southern part of the SSFL, suggesting that it is a relatively continuous structure. The gouge and fracture characteristics of the fault could not be evaluated because of a lack of exposures.

- **Shear Zone:** The Shear Zone is interpreted to be a continuous feature on the basis of a well-defined topographic low along the trace of the structure. It shows significant gouge development, with gouge zones locally being more than 1.5 feet thick. The Shear Zone is exposed at four locations within the SSFL and at each of these locations it shows a 40 to 50 foot wide zone of closely fractured rock.

- **Skyline Fault:** The Skyline Fault is characterized by a well-developed air photo lineament, suggesting that it is a relatively continuous feature. Existing exposures of the Skyline Fault are poor and very sparse, but they suggest that there is little, if any, gouge and that there is no significant fracturing adjacent to the fault zone.

Joints at the SSFL typically strike either to the north-northwest or to the northeast, with most of the northeast striking joints being in the southern and eastern part of the site. Joint spacing varies from 15 feet to more than 1,000 feet within SSFL. In general, joints are more closely spaced within Sandstone 1 than within Sandstone 2 and are confined within a single sandstone bed.

3.5 Preliminary Assessment of the Effects of Geologic Features on Groundwater Flow

The evaluation of the geologic framework at the SSFL resulted in some general observations about the potential impacts of the site geology on the fracture network and groundwater flow. These general observations include:

- The finer-grained lower Chatsworth Formation is expected to influence groundwater flow in the eastern part of the SSFL.

- The lower permeability of the through-going shale units (Shale 2 and 3) in the upper Chatsworth Formation is expected to slow the flow of groundwater across these features.

- The significant gouge present at the Shear Zone is also expected to slow the flow of groundwater across it.

- The lenticular deposition of the sandstone beds coupled with joints that are confined to a single sandstone bed likely result in circuitous groundwater flow paths and an interconnected fracture networks as observed at a number of outcrop locations at the SSFL.

Further discussions of the site geology on the fracture network and groundwater flow will be discussed in more detail in subsequent sections of this technical memorandum.

HDMSe00012899

4.0 Hydrogeology

The discussion of the hydrogeologic setting of the SSFL includes a historical summary of groundwater usage, discussion on the hydraulic parameters of the Chatsworth Formation, the effects of stratigraphy and geologic structures on the groundwater flow and an assessment of the connectivity of the fracture network. A detailed description of the hydrogeology is provided in Appendix B.

4.1 Historical Summary

Water supply development activities at the Santa Susana site began in 1948 with the initiation of the Propulsion Field Laboratory on 430 acres now known as Area I (Rocketdyne, 1963). Wells were installed to meet the water resource needs for the expanding test facility, which by 1954 had grown to 1,526 acres. By 1963, 17 water supply wells had been installed in the Chatsworth Formation, but only 6 of the wells yielded sufficient water and the remainder were abandoned or not used. Total groundwater withdrawal from the six wells remaining peaked at 400 gallons per minute (gpm) in 1958, and averaged about 250 gpm between 1956 and 1963. Water usage during this period was primarily for cooling purposes during rocket testing. This rate of pumping resulted in the dewatering of the Chatsworth Formation groundwater in the central portion of the site, with over 500 feet of water level decline observed by the early 1960s. This significant dewatering, coupled with the expanding water demand necessary to support testing for the rocket engine program, resulted in the construction of a water supply pipeline to the Calleguas Water District in 1963. Groundwater extraction was minimal during the late 1960s, and no groundwater pumping was reported from 1970 to 1984.

Investigation of groundwater quality in the Chatsworth Formation began at the site in 1984 with the installation of bedrock monitoring wells. The identification of impacted groundwater resulted in the re-activation of two water supply wells in 1984 (WS-5 and WS-6), with pumping from additional water supply and monitoring wells initiated in the late 1980s and early 1990s. Groundwater withdrawal averaged about 100 gpm between 1984 and 1988, and has averaged about 250 gpm since that time, with the treated water discharged to streams and ponds on the site. This treated water is believed to provide a source of recharge to the underlying groundwater system.

The current water level decline resulting from groundwater pumping has been limited to about 250 feet in the central portion of the SSFL.

Water importation from the Calleguas Water District has continued to the present time at an annualized average rate ranging from about 50 to 130 gpm, providing a total water supply at SSFL of 300 to 350 gpm.

4.2 Estimate of Site Bulk Hydraulic Conductivity

David McWhorter of the Expert Panel initially observed that the water table and the geographic setting at the SSFL should result in a low bulk hydraulic conductivity. The low bulk hydraulic conductivity was expected because the SSFL sits atop the Simi Hills with valleys to the north and south and yet the water table of the Chatsworth Formation is near the ground surface (between 10 and 80 feet below ground surface in areas that are outside of the influence of groundwater extraction wells).

A conceptual water balance was performed to estimate the site-wide bulk hydraulic conductivity of the Chatsworth Formation (Figure 4.1). The bulk hydraulic conductivity estimate is based on the height and geometry of a groundwater mound beneath the site and the average recharge rate. For this estimate, the water table beneath the SSFL was modeled as a dome and a ridge. Recharge was estimated to range from 10 to 20 percent of annual precipitation, which is about 20 inches per year. Using a recharge rate of 10 percent, the estimated bulk hydraulic conductivity is 1.25×10^{5} centimeters per second (cm/sec) for the dome configuration and 2.5×10^{5} cm/sec for the ridge. Increasing the recharge rate to 20 percent results in bulk hydraulic conductivity estimates of 2.5×10^{5} and 5×10^{-5} cm/sec, for the dome and ridge, respectively.

HDMSe00012900

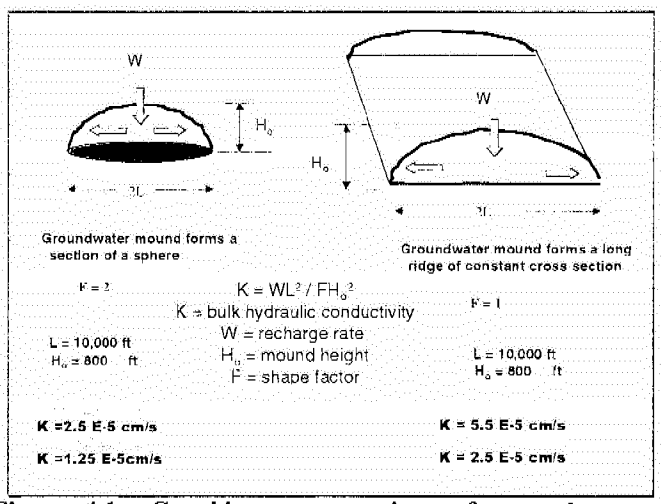

Figure 4.1 Graphic representations of groundwater mounds beneath the SSFL. The formula used to calculate the site-wide bulk hydraulic conductivity and the results of the calculations are shown.

The bulk hydraulic conductivity (K_b)of the Chatsworth Formation was also estimated using data collected from packer testing in two open boreholes and from pumping tests on completed wells. Estimates of the bulk hydraulic conductivity from each of these two sets of data are summarized below.

- **Packer Tests:** Packer testing was conducted at RD-35B and RD-46B to aid in the selection of screened intervals for these two boreholes. Eleven different zones were tested using straddle-packers. The results of these tests indicate that the bulk hydraulic conductivity ranged from 10^{-7} cm/sec to 10^{-1} cm/sec, with a geometric mean of 4.5 x 10^{-5} cm/sec (see Figure 4.2 for distribution of K_b). The geometric mean is consistent with the bulk hydraulic conductivity determined from the water balance

- **Pumping Tests:** Pumping test data from a combination of 87 monitoring and water supply wells were analyzed to evaluate the bulk hydraulic conductivity. Interpretation of the pumping test data indicates that the bulk hydraulic conductivity of the Chatsworth Formation ranges from 10^{-7} to 10^{-1} cm/sec, with a geometric mean of 1.3 x 10^{-5} cm/sec (see Figure 4.3 for distribution of K_b). The geometric mean is also consistent with the bulk hydraulic conductivity estimated from the water balance. The pumping test results were also reviewed within the context of the site stratigraphy. This review indicates that the bulk hydraulic conductivity of Sandstone 1 (geometric mean of 3.4 x 10^{-5} cm/sec) is approximately an order-of-magnitude higher than Sandstone 2 (geometric mean of 4.2 x 10^{-6} cm/sec). It is important to note that the bulk hydraulic conductivity estimates from pumping tests are biased high. The high bias is the result of the well installation method and the fact that low conductivity zones are not tested due to the lack of water production.

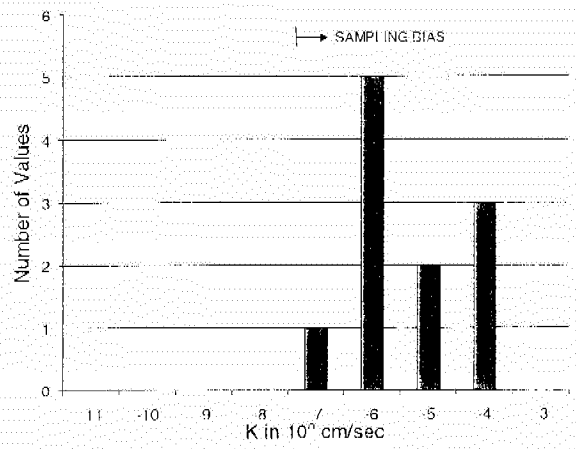

Figure 4.2 Frequency plot of estimates of bulk hydraulic conductivity from straddle packer tests at RD35B and RD46B.

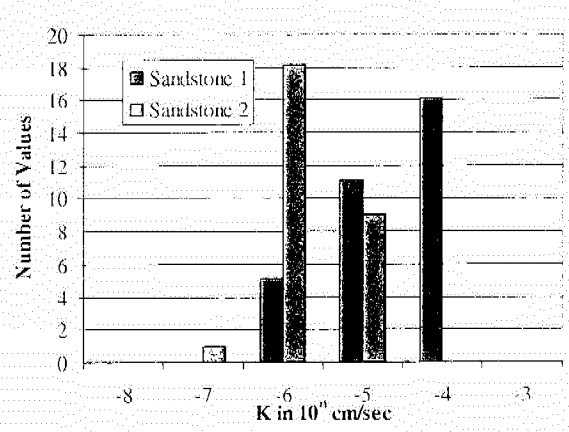

Figure 4.3 Frequency plot of estimates of bulk hydraulic conductivity in Sandstones 1 and 2. Estimates are from analysis of pumping test data.

4.3 Matrix Hydraulic Conductivity

The hydraulic conductivity of the rock matrix was determined through laboratory analysis of 21 samples of rock core from boreholes drilled at the SSFL. Values ranged from 8.5 x 10^{-11} to 1.7 x 10^{-4} cm/sec. The geometric mean matrix hydraulic conductivity is 1.7 x 10^{-6} cm/sec. The matrix hydraulic conductivity is about one order-of-magnitude lower than the bulk hydraulic conductivity of the Chatsworth Formation as estimated from the water balance and pumping tests, indicating that the hydraulic conductivity of the formation is dominated by the fractures within the bedrock.

HDMSe00012901

4.4 Vadose Zone Water Content

The water content of the Chatsworth Formation vadose zone was estimated using two different approaches.

- **Direct Measurement:** Laboratory measurements of water content were made on four rock core samples from the vadose zone at RD-46B. The mean value of these four measurements was 73% of the pore volume.

- **Estimate Using Empirical Formulas:** The water content of the vadose zone can be calculated if the recharge flux and saturated matrix hydraulic conductivity are known. Estimates of recharge are as presented in section 4.2. Assuming that recharge occurs uniformly over the entire site, 10% recharge equates to a flux of 1.6×10^{-7} cm/sec and 20% recharge equals a flux of 3.2×10^{-7} cm/sec. As presented in section 4.3, the geometric mean hydraulic conductivity of the matrix is estimated to be 1.7×10^{-6} cm/sec. This recharge flux is lower than the matrix hydraulic conductivity by a factor ranging from 5 to 10 times, depending upon the assumed recharge rate. This indicates that under normal recharge conditions the vadose zone is not fully saturated. Calculations using the empirical relationship, shown in Table 4.1, indicate that the water content of the vadose zone should be approximately 70% of the pore volume. This result is very close to the vadose zone water content determined through laboratory measurements.

$$W = K_m K_r$$

W = recharge flux
K_m = saturated matrix hydraulic conductivity
K_r = relative permeability in the matrix
Relative permeability in Matrix = 0.2

Typical Relationship : $K_r = S_w^4$
K_r = relative permeability in the matrix
S_w = water saturation in the matrix
Water saturation in the Matrix = 0.7

Table 4.1 Equations and calculations of relative permeability of matrix to water and water saturation

4.5. Influence of Stratigraphy and Geologic Structure on Bulk Hydraulic Conductivity

The analysis of the SSFL geology that was presented in section 3.0 indicated that the through-going shale units and the Shear Zone were likely to restrict the flow of groundwater across these units. These preliminary conclusions, along with an evaluation of groundwater flow across other geologic structures, are more fully developed as follows.

Effects of Shale Units

As mentioned in Section 4.3, hydraulic conductivity measurements were made on 21 samples of rock core. Three of the 21 samples were collected from shale units and had hydraulic conductivities ranging from 8.5×10^{-11} to 6.4×10^{-9} cm/sec. These results are between 3 and 5 orders-of-magnitude lower than the hydraulic conductivity of the remaining 18 sandstone samples. This reduced hydraulic conductivity is expected to restrict the flow of groundwater across the shale units as described below.

- **Shale 2:** Shale 2 acts as an aquitard between Sandstone 1 and Sandstone 2. The behavior of Shale 2 as an aquitard is demonstrated by the observed water level offsets across Shale 2 as shown on Figure 4.4. Groundwater extraction within Sandstone 1 (discussed in section 4.1) has resulted in a reduction in the water levels within Sandstone 1 by approximately 250 feet, while the water levels in Sandstone 2 remain virtually unaffected since little groundwater has been withdrawn from this stratigraphic unit. Additionally, hydraulic stimuli induced within Sandstone 1 are not transmitted through Shale 2 and do not impart a hydraulic response in groundwater within Sandstone 2.

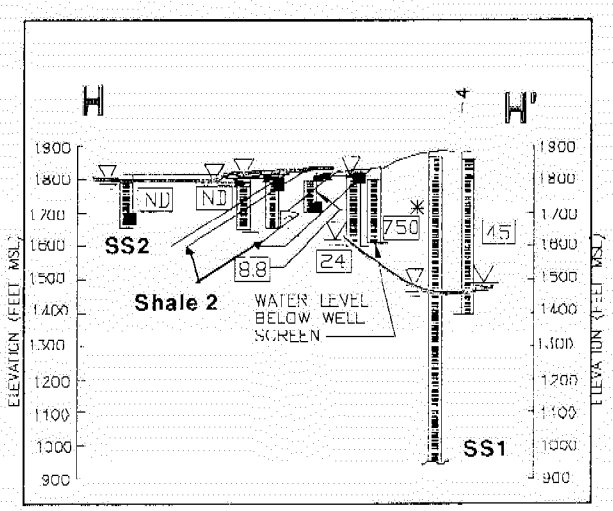

Figure 4.4 Water Level Offsets Across Shale 2. Depressed water levels in Sandstone 1 are produced by significant groundwater withdrawals.

HDMSe00012902

- Shale 3 acts as an aquitard between Sandstone 2 and the Simi Conglomerate Member of the Santa Susana Formation. The effects of the low permeability of Shale 3 can be seen on Figure 4.5 showing artesian conditions in wells screened through Shale 3 and into Sandstone 2.

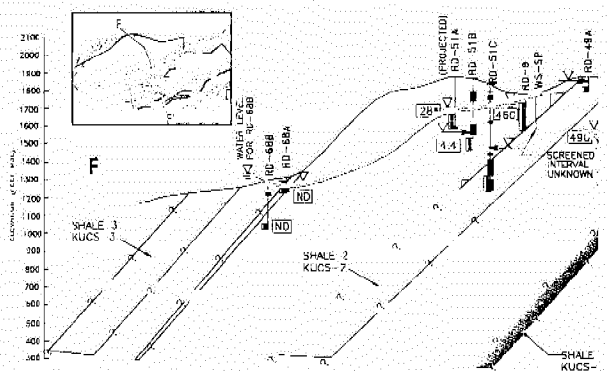

Figure 4.5 Artesian conditions produced at wells screened in Sandstone 2 just beneath Shale 3.

- **Happy Valley Shale:** Analysis using water elevation correlations between well pairs located on either side of the Happy Valley Shale indicates that this shale unit also acts as an aquitard.

Effects of Faults

The Shear Zone appears to act as an aquitard, most likely due to the wide gouge zone. Evidence supporting this conclusion includes:

- Significant offset in water levels across the Shear Zone which is shown on Figure 4.6,

- Lack of response to hydraulic stimuli induced by pumping across the Shear Zone associated with long term groundwater extraction and a hydraulic communication study, and

- Little correlation in water elevations between well pairs located on either side of the Shear Zone .

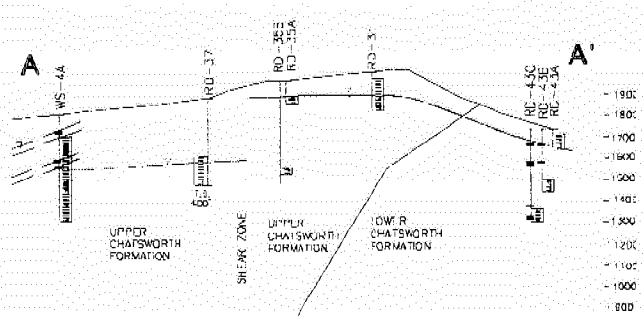

Figure 4.6 Water level offset across the Shear Zone. The water level offset, which is almost 300 feet is produced by groundwater extraction from wells in Sandstone 1 located west of the Shear Zone.

A similar analysis indicates that the Coca Fault also likely acts as an aquitard although the data supporting this conclusion are not as definitive as that across the Shear Zone because there are few wells located immediately north of the Coca Fault.

Analysis of Variations in Hydraulic Conductivity of Wells Placed on Faults

The potential that wells constructed along major fracture zones at SSFL are zones of increased hydraulic conductivity (i.e. preferential groundwater flow paths) was evaluated as described below.

- The bulk hydraulic conductivity from wells placed on faults within Sandstone 1 was compared to those of wells not placed on faults. Hydraulic conductivities were calculated from pumping tests on 33 wells within Sandstone 1. Nine of the 33 wells are located on major faults or lineaments. The geometric mean hydraulic conductivity for wells installed on fault lineaments was 1.4×10^{-5} cm/sec, while the corresponding geometric mean hydraulic conductivity for wells not installed along faults was 4.4×10^{-5} cm/sec. This indicates that these faults or lineaments are not preferred groundwater flow paths. Additionally, when the hydraulic conductivity of wells across the site is considered, the wells with the highest hydraulic conductivity are most often located off of faults or lineaments.

- The lack of increased hydraulic conductivity along faults in the Chatsworth Formation is also supported by the fact that the majority of the 17 water supply wells installed by 1963 were abandoned because of low yield, even though most of these wells were specifically located in or on fault lineaments.

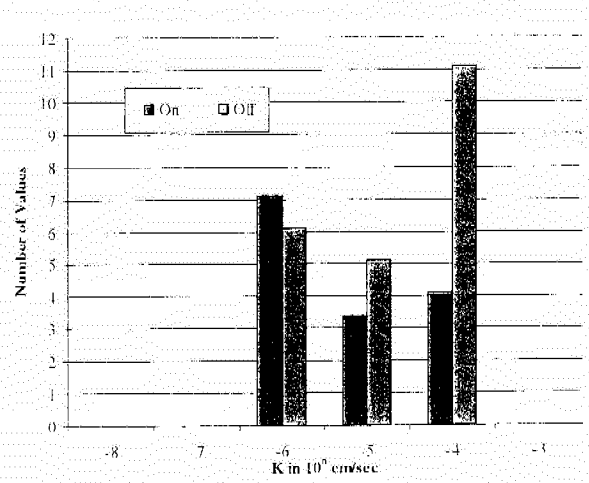

Figure 4.7 Frequency plots of bulk hydraulic conductivity of wells in Sandstone 1 placed on and off lineaments.

HDMSe00012903

4.6 Delineation of Groundwater Units

The presence and hydraulic characteristics of Shale 2, Shale 3 and the Happy Valley Shale and the Shear Zone and Coca Fault result in compartmentalizing the groundwater system into five distinct units as shown on Figure 4.8.

4.7 Interconnected Nature of Chatsworth Formation Fracture Network

The fractures present within the sandstone and shale units of the Chatsworth Formation join to form an interconnected network within each of the groundwater units. This interconnected fracture network imparts an order-of-magnitude increase in the bulk hydraulic conductivity over the sandstone matrix that comprises the Chatsworth Formation and dominates groundwater flow.

Evidence of the interconnected fracture network can be found in:

- Observations of fracture patterns and connections in rock outcrop and in aerial photos,
- Fracture patterns within downhole geophysical and video logs of boreholes,
- Hydraulic responses in water level changes observed during multi-well pumping tests,
- Site-wide response in water level changes to long-term groundwater extraction, and
- Correlations of water elevation changes between well pairs within groundwater units over long distances.

4.8 Groundwater Flow Within Groundwater Units

A preliminary understanding of the groundwater flow within each of the five groundwater units has been developed by reviewing well construction details, water levels, and hydraulic head and conductivities within the context of the site geology. This review has resulted in the following general conclusions about groundwater flow at the SSFL:

- Groundwater flow and hydraulic head profiles are strongly influenced by the presence and distribution of lithologic units within the Chatsworth Formation that have both higher and lower hydraulic conductivities. Analysis of the pumping and packer test data has shown that both the lateral and vertical distribution of hydraulic conductivity at the SSFL ranges by over four orders-of-magnitude (10^{-7} through 10^{-3} cm/sec).
- The location of the lithologic units with lower hydraulic conductivities, such as the shale units previously discussed in this section, likely result in shallow groundwater circulation that directs the discharge of groundwater toward the northern and southern slopes of the Simi Hills.
- Variability of fracture apertures and spacing within the fracture network can produce strong local upward or downward hydraulic gradients.
- Monitoring wells with long open intervals provide water levels that are blended values of head from various depths within the well.

Figure 4.8 Geologic structures and stratigraphy compartmentalize groundwater flow at the SSFL. Five groundwater units have been established based upon analysis of hydrogeologic data.

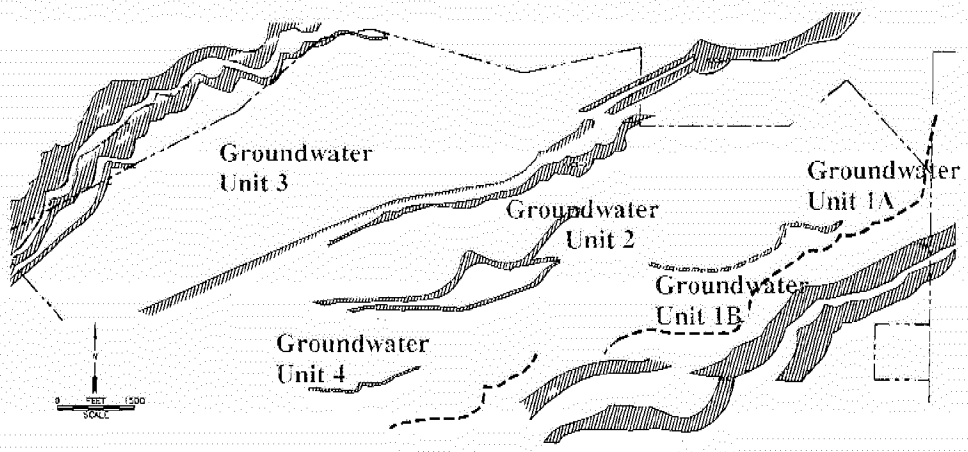

HDMSe00012904

A brief discussion of groundwater flow within each of the five-groundwater units is presented below. The water table surface is shown on Figure 4.9. The water table surface was constructed using wells with fairly short open intervals (i.e., less than 75 feet) and using only these wells that intercept the water table. Deeper wells associated with well clusters were not used to construct the water table surface.

- **Groundwater Unit 1A**: Groundwater flow appears to be primarily to the northeast parallel to the Shear Zone and the strike of the Chatsworth Formation. Most flow likely occurs in the upper few hundred feet of bedrock because of the presence of low permeability strata at depth (likely the Happy Valley Shale). The estimated rate of groundwater discharge to the northeast is approximately a few gpm, based on the observed groundwater gradient (0.001 feet per feet (ft/ft)) and average bulk hydraulic conductivity.

- **Groundwater Unit 1B**: Groundwater flow appears to be primarily to the northwest and is influenced by pumping from wells RD-1, RD-2 and possibly WS-5.

- **Groundwater Unit 2**: Flow directions are dominated by pumping from several wells located in the central portion of the site (WS-6 and RD-4). As a result, the apparent direction of groundwater flow is toward these wells. Groundwater recharge is evident along the western boundary of the unit formed by Shale 2, coincident with the location of surface water storage ponds.

- **Groundwater Unit 3**: The primary direction of groundwater flow is to the north and northwest. The lower bulk hydraulic conductivity of this groundwater unit that is within Sandstone 2 produces a steeper groundwater gradient, as the elevation in the northwest drops rapidly. The estimated rate of groundwater discharge along the northern boundary of the unit ranges between 5 and 10 gpm based on the observed groundwater gradient (0.18 ft/ft) and bulk hydraulic conductivity.

- **Groundwater Unit 4**: Flow is primarily to the south from the Coca Fault and is influenced by extraction from well WS-9A, which appears to capture groundwater in the western portion of the unit. Major shale units of the lower Chatsworth Formation occur in the eastern half of the unit, and may act to further influence groundwater flow.

4.9 Hydraulic Fracture Apertures, Fracture Porosity and Average Linear Groundwater Velocity

The hydraulic aperture of the fractures in the bedrock can be calculated using the Cubic Law (Snow, 1968), which relates bulk hydraulic conductivity, fracture spacing and fracture aperture according to the following formula:

$$K = (1/L_1 + 1/L_2)\,\varepsilon^3\,\gamma\,/12\,\mu$$

where L_1 and L_2 are the fracture spacings in the x and y directions, ε is the fracture aperture, γ is the specific weight of water and μ is the viscosity of water. Hydraulic fracture apertures were estimated using two different sets of data representing spatial scales that range from local (at RD-35B and RD-46B) to site-wide, each discussed below.

- **Double-packer Tests at RD-35B and RD-46B**: Hydraulic apertures were calculated from bulk hydraulic conductivity values that were determined from various pumping tests conducted within these two boreholes. The number of open fractures that intercepted the borehole within the tested interval was also counted. Calculations showed the hydraulic apertures ranged from 10 to 299 microns. Details of the approach taken are provided in Appendix C.

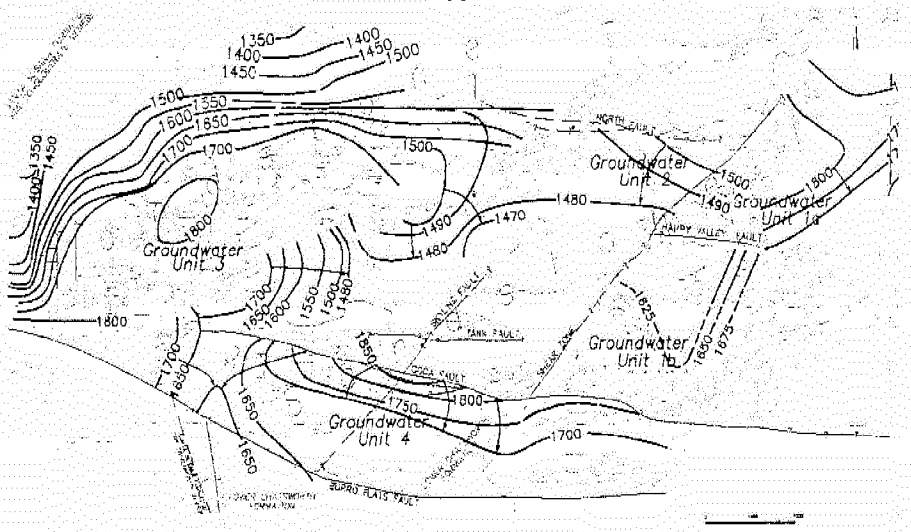

Figure 4.9 Chatsworth Formation Water Table Surface Map

HDMSe00012905

- Water Balance: The site-wide bulk hydraulic conductivities that were derived from the water balance were used along with fracture spacings of one to ten meters and spacing geometries of cubes and infinite parallel plates, which represent end members of the spacing between fractures. The hydraulic apertures calculated using this approach ranged from 40 to 180 microns.

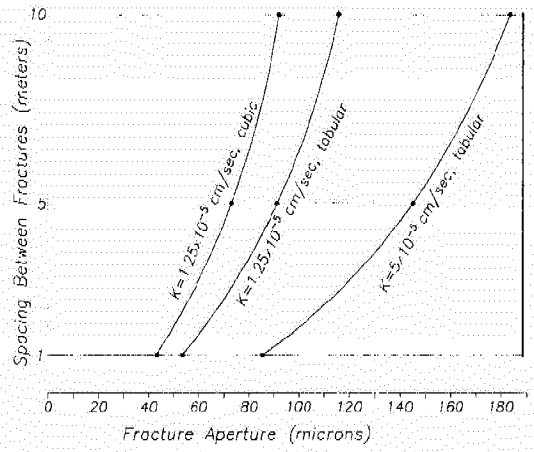

Figure 4.10 Graph of hydraulic fracture apertures as a function of spacing between fractures, type of fracture patterns (cubic or tabular) and different hydraulic conductivities from site-wide water balance.

The porosity of the fracture network was calculated based on ranges of the observed fracture spacing at the SSFL and a hydraulic fracture aperture of 50 microns. These calculations show that the fracture porosity of the Chatsworth Formation is very small (1×10^{-4} to 5×10^{-6} or 0.01% to 0.0005%). Conversely, the porosity of the rock matrix averages about 0.13 or 13% based on laboratory measurements from 59 rock core samples.

For An Aperture of 50 microns			
Cubic Matrix Blocks		***Tabular Matrix Blocks***	
Fracture Porosity = 3 ε / L		Fracture Porosity = ε / L	
Spacing - meters	Fracture Porosity	Spacing - meters	Fracture Porosity
1	1.5 E-4	1	5.0 E-5
5	3.0 E-5	5	1.0 E-5
10	1.5 E-5	10	5.0 E-6

Table 4.2 Estimate of fracture porosity for a fracture aperture of 50 microns.

Ranges of the average linear groundwater velocity can be calculated using the bulk hydraulic conductivity, groundwater gradient and fracture porosity that have been estimated by using the following formula:

$$\psi = \frac{K_b(i)}{\phi_f}$$

where:

ψ = average linear groundwater velocity
K_b = bulk hydraulic conductivity
i = hydraulic gradient
ϕ_f = fracture porosity

These calculations show that the average linear groundwater velocity at SSFL ranges from 500 to 10,000 feet per year. The actual groundwater velocities are expected to be larger than the average linear groundwater velocity because the actual flow paths will be much longer.

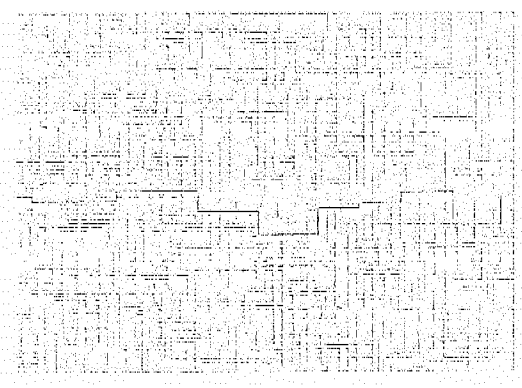

Figure 4.11 Conceptual depiction of average linear groundwater velocity.

4.10 Summary of Hydrogeology at the SSFL

A summary of the hydrogeologic parameters that have been measured, calculated or estimated for the SSFL is provided in Table 4.3.

These data have been used to characterize various aspects of the hydrogeologic system at the SSFL and have resulted in the following conclusions:

- The recharge flux is less than the saturated matrix hydraulic conductivity and indicates that the bulk matrix is unsaturated on average. The recharge flux is also less than the bulk hydraulic conductivity, which indicates that the fractures in the vadose zone are not water filled under average conditions.

HDMSe00012906

- The average bulk hydraulic conductivity of the site is approximately an order-of-magnitude greater than the matrix hydraulic conductivity indicating that groundwater flow is predominately through an interconnected fracture network. However, water storage is dominated by the porosity provided by the matrix (about 13%) and not the fracture network, since the fracture porosity is four to six orders-of-magnitude lower than the matrix porosity.

- Hydraulic fracture apertures are small and average about 70 microns on a site-wide basis. The fracture network is interconnected based on outcrop and aerial photo observations, downhole geophysical tests and water level responses from various pumping tests.

- The average bulk hydraulic conductivity of the site is low. Calculations made using the site-wide water balance show the bulk hydraulic conductivity ranges between 1.25×10^{-5} cm/sec to 5.0×10^{-5} cm/sec. The average bulk hydraulic conductivity from numerous pumping tests performed at the SSFL is 1.7×10^{-5} cm/sec. The hydraulic conductivity calculated from the pumping tests are biased high, as many of the wells with lower hydraulic conductivity were not tested. Additionally, the methods used for well installation result in biasing the hydraulic conductivity high.

- An evaluation of the hydraulic conductivity of wells placed on lineaments against those not place on lineaments did not reveal any systematic increase in hydraulic conductivity of wells placed on lineaments. These data have been used to conclude that lineaments are not preferred groundwater flow paths.

- Although the average linear groundwater velocities are high (hundreds to thousands of feet per year), the volumetric discharge of groundwater (a few to tens of gallons per minute) from the site is low because of the low average bulk hydraulic conductivity.

- Depth-discrete hydraulic head profiles are strongly influenced by beds of low and high hydraulic conductivity. The head profiles also vary significantly depending on the details of the fracture network. These variations produce a three-dimensional network of hydraulic head that greatly influences the flow of groundwater at the SSFL.

- Groundwater withdrawals at the SSFL have produced water level off-sets across stratigraphic units and geologic structures. The through-going shale units and a few of the faults are aquitards and groundwater movement across these features is restricted. The flow of groundwater at the SSFL is compartmentalized by the lower permeability of shale units and some faults.

	No. of Measurements	*Minimum*	*Maximum*	*Average*
Vadose Zone Water Content				
• ***Laboratory Measurements***	4	0.52	0.84	0.73
• ***Calculated***	NA	NA	NA	0.70
Matrix Hydraulic Conductivity (cm/sec)				
• ***All Samples***	21	8.5×10^{-11}	1.7×10^{-4}	1.7×10^{-6}
• ***Shale***	3	8.5×10^{-11}	6.4×10^{-9}	2.2×10^{-9}
Matrix Porosity (%)	59	1	21.6	13
Bulk Hydraulic Conductivity (cm/sec)				
• ***Site Wide Water Balance***	NA	1.25×10^{-5}	5.0×10^{-5}	NA
• ***Pumping Tests***	101	5.9×10^{-7}	2.7×10^{-3}	1.3×10^{-5} (geometric mean)
✓ ***Sandstone 1***	41			3.4×10^{-5} (geometric mean)
- ***Sandstone 1, Wells On Lineaments***	14	$<1.0 \times 10^{-6}$	9.0×10^{-4}	1.4×10^{-5} (geometric mean)
✓ ***Sandstone 2***	38	5.9×10^{-7}	3.4×10^{-5}	4.2×10^{-6} (geometric mean)
✓ ***Lower Chatsworth Formation***	8	$<1.0 \times 10^{-6}$	2.7×10^{-3}	2.7×10^{-5} (geometric mean)
Recharge Flux Provided by Precipitation (cm/sec)	NA	1.6×10^{-7}	3.2×10^{-7}	NA
Hydraulic Fracture Apertures				
• ***Local Scale RD-36B and RD-46B***	32	10	299	70 (geometric mean)
• ***Site-Wide Scale, from water balance***	NA	40	180	NA
Fracture Porosity (%) (from site-wide water balance)	NA	0.0005	0.01	NA
Average Linear Groundwater Velocity (ft/yr)	NA	500	10,000	NA

Table 4.3 Summary of Hydraulic Parameters - Ranges of Values NA = not applicable

HDMSe00012907

5.0 TCE Occurrence at the SSFL

This section discusses TCE input locations at the SSFL, preliminary RCRA Facility Investigation (RFI) findings in alluvial soils at these locations, and correlates these findings with the presence and concentration of TCE in Chatsworth Formation groundwater.

5.1 TCE Input Locations

TCE was used primarily at four types of facilities at the SSFL. These facilities included rocket engine test stands, component test laboratories, support laboratories, and other facilities. These operations were conducted at a number of locations and are further described below. Additional descriptions can also be found in Appendix C of the RFI Field Sampling Plans (Ogden, 1996).

- **Rocket Engine Test Stands** – Six test stands have been used for rocket engine testing at the SSFL and include: Bowl, Canyon, Alfa, Bravo, Coca and Delta, and of these only Alfa and Bravo are still active. Locations are shown on Figure 5.1. TCE was used at these locations to rinse the rocket engines of hydrocarbons after test firing. Until the early 1960s, TCE was released to the test stands' concrete aprons approximately 70 feet below the suspended rocket engine and either evaporated at the test stand or drained to ponds. A TCE recycling system was installed at the test stands in 1961. TCE use was discontinued in 1994.

- **Component Test Laboratories** – Five component test laboratories (CTLs) were used at the SSFL and only three of these (CTL-II, CTL-III and CTL-IV) were reported to have used significant quantities of TCE. TCE use was similar to that for the rocket engine test stands, except much smaller equipment was rinsed. At these three CTLs, TCE was typically discharged to concrete surfaces and then rinsed to ponds. CTL-II is now referred to as ELV (Expendable Launch Vehicle) and CTL-IV is now referred to as STL-IV (Systems Test Laboratory).

- **Support Laboratories** – Two support laboratories, Instrument and Equipment Laboratory (IEL) and Engineering Chemistry Laboratory (ECL), provided support for the various test areas. The IEL was used for rocket engine equipment assembly and preparation, and had multiple solvent use or handling areas (aboveground and underground storage tanks, clarifiers and distillation units). The ECL was used to prepare some of the chemicals used for testing at the SSFL and used a large quantity of solvents. Wastes at ECL were discharged to ponds.

- **Other Significant TCE Use Areas** - Three facilities also reportedly used or handled significant quantities of solvents. The Advanced Propulsion Test Facility (APTF) is a test area that used TCE for cleaning purposes. The Former Sodium Disposal Facility (FSDF) and the Area 1 Thermal Treatment Facility (TTF) were used for chemical treatment and disposal. Both the FSDF and the TTF typically discharged waste solvents to ponds or pits.

The RFI has been investigating impacts of chemicals to the subsurface at a total of 39 sites that are located throughout the SSFL. Of the sites described above, the TTF is not considered an RFI site. It is a permitted unit and is included in this discussion because of elevated TCE findings at this facility. Results from the RFI also identified the presence of elevated TCE at four other areas at the SSFL: the Compound A Facility, the former Liquid Oxygen (LOX) Facility, the Environmental Effects Laboratory (EEL), and the Sodium Reactor Experiment (SRE). The past use of TCE at these facilities is unknown.

5.2 Historical and Preliminary RFI Findings

Field investigations completed during the RFI included sampling and analysis for the presence of TCE in sediment, soil, soil vapor, and groundwater. The RFI samples were collected where alluvial soils are present and that occur mainly in site drainages. The alluvial soils are typically 3 to 15 feet thick, but locally reach thicknesses up to 40 feet.

Field action levels for TCE in soil and soil vapor were developed during RFI planning. The field action level (FAL) for TCE in soil vapor is 100 micrograms per liter by volume (ug/L_v), and 190 micrograms per kilogram (ug/kg) in soil. A report on the preliminary RFI results of soil sampling was issued (Ogden, 1999) and can be reviewed to develop a more thorough understanding of the results. These results were used to identify areas at each of the input locations where TCE was detected above the FALs. As expected, the results generally show a positive correlation between TCE input locations and TCE occurrence in the subsurface. Locations where TCE was detected above the field action levels and the highest concentrations detected at each location are shown on Table 5.1.

HDMSe00012908

Input Location	SWMU or AOC No.	Maximum Detected TCE Concentration[a]	
		Soil Vapor (ug/L_v)	Soil (ug/kg)
Test Stands			
Bowl	4.15	41	ND
Canyon	4.14	3	56
Alfa	5.9/10/11	65,000	910,000
Bravo	5.13/14/15	1,600	270
Coca	5.18/19	2.8	360
Delta	5.23/24/25	31	*84,000*
CTLs			
ELV (CTL II)	5.2	3,200	33,000
CTL-III	4.7	7,600	230
STL-IV(CTL IV)	6.5/6/7	310	*180*
Support Labs			
IEL	4.3/4	2,800	5,600
ECL	6.1/2/3	120	19
Others			
LOX	4.5	ND	*470*[b]
APTF	4.9/10/11	1,100	200
Compound A	6.4	1,500	84
EEL	6.9	120	ND
FSDF	7.5	NA	*740,000*
SRE	Area IV AOC	ND	1,000
TTF	4.8	NA	*190,000*

Table 5.1

ug/L_v = micrograms per liter by volume
ug/kg = micrograms per kilogram
NA = not analyzed ND = not detected
SWMU = Solid Waste Mangement Unit AOC = Area of Concern
Italics = soils/sludge removed from site
(a) Maximum TCE concentration reported in Ogden (1999), ICF Kaiser (1993 a-c) or GRC (1993). Values in italics indicate soils/sludges have been removed from site.
(b) Micrograms per liter, detected in clarifier/sump liquid contents.

5.3 TCE in Chatsworth Formation Groundwater

A map of the dissolved concentrations of TCE in Chatsworth Formation groundwater from samples collected during 1998 was developed and is presented in Figure 5.1. The data presented in the figure uses the highest TCE concentration detected in groundwater during 1998 for each well location sampled. Isoconcentration contours were also developed and are presented on the figure. Contour lines are plotted for areas interpreted to contain TCE concentrations in Chatsworth Formation groundwater that are:

- equal to or exceed 1 milligram per liter (mg/L),
- less than 1 mg/L, but greater than or equal to 0.1 mg/L and,
- less than 0.1 mg/L, but greater than or equal to 0.005 mg/L.

Some boundaries of the isoconcentration contours are the result of the hydrogeologic analysis presented in section 4.0. This analysis discusses the presence of aquitards that compartmentalize groundwater flow and thus TCE transport. The figure also identifies the areas where the FALs were exceeded at each of the input locations discussed in section 5.2.

With few exceptions, the presence of TCE in alluvial soils correlates well with the presence and concentration of TCE in Chatsworth Formation groundwater. Investigation of potential source areas for observed impacts in Chatsworth Formation wells is continuing at the Building 56 Landfill, STL-IV, LOX, Canyon, and Bowl sites.

Additionally, inspection of the isoconcentration contours indicates that the highest concentrations of TCE in groundwater are near the input locations. Inspections of the data also indicate that the leading edges (defined as TCE concentrations exceeding 0.005 mg/L) of the TCE plumes are within hundreds to a few thousands of feet within the input locations.

HDMSe00012909

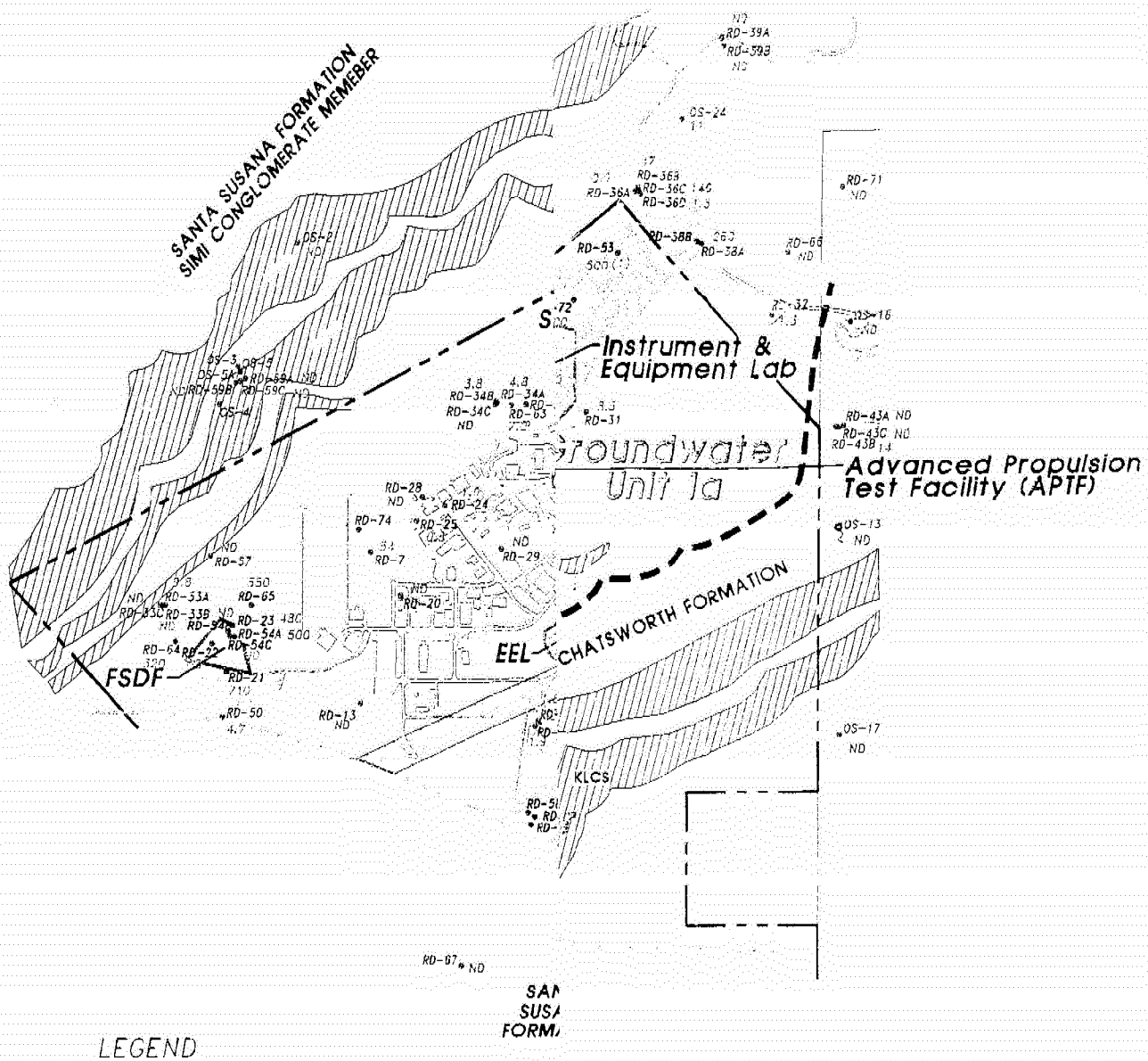

LEGEND

PROPERTY BOUNDARY

SHALE BED

MAJOR FAUL

MINOR FAUL

PERMITTED F

APPROXIMATE (SOIL VAPOR

APPROXIMATE (REMOVED S

TCE IN GROU >1,000 ug/

TCE IN GROU >100 <1,00

TCE IN GROU >5 <100 u

500 TCE CONCEN

RD-29 CHATSWORT

OS-12 SPRING LOC

NTGOMERY WATSON

DYNE PROPULSION & POWER
SUSANA FIELD LABORATORY
MI VALLEY, CALIFORNIA

NPUT LOCATIONS & TCE
ION IN ALLUVIAL SOILS AND
TH FORMATION GROUNDWATER

FIGURE 5.1

JOB No. ___ FILE No. ___ D:\PROJECTS\

6.0 Flow, Distribution and Fate of TCE DNAPL in Source Zones

An overview of TCE DNAPL flow, distribution and fate, along with the timeframes over which this process is expected to occur is presented below. In summary, four stages of DNAPL movement have been identified and are described below. The development of TCE plumes is also briefly discussed below and will be more fully evaluated in section 7.0.

Stage 1: ***DNAPL entry and flow into the fractured sandstone (Figure 6.1).*** TCE DNAPL preferentially entered the fractures and spontaneously imbibed into the unsaturated portions of the rock matrix. DNAPL flowed within the fractures until its mass was depleted. If sufficient mass was present, or repeated release events occurred, the DNAPL continued to flow within the fracture network through the vadose zone and into the saturated zone where its flow was stopped by a number of processes. The timeframe over which DNAPL entry and flow is believed to have occurred at the SSFL is months to tens of years. This aspect of DNAPL movement is more fully discussed in sections 6.1, 6.3 and 6.4.

Figure 6.1

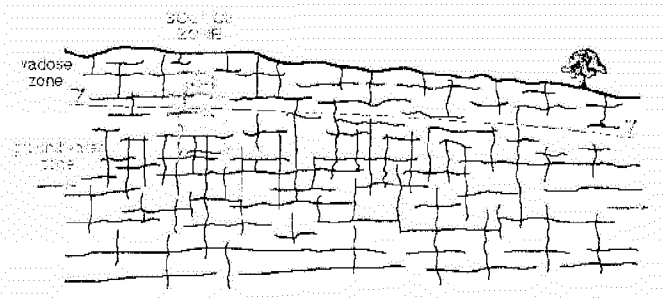

Stage 1: DNAPL Enters and Flows in Fractured Sandstone

Stage 2: ***DNAPL immobility and dissolution (Figure 6.2).*** After releases have stopped, the DNAPL stopped flowing and reached equilibrium within the fracture network as either a liquid within the unsaturated rock matrix or as a liquid within the fracture network. At that point, DNAPL present within the fractures of the saturated rock started to dissolve into the groundwater as governed by its aqueous solubility. The timeframe for this process ranged from months to tens of years. The time lag between DNAPL release into the subsurface and its immobility is dependent on the mass loading of DNAPL, but is generally expected to have ranged from months to tens of years.

Figure 6.2

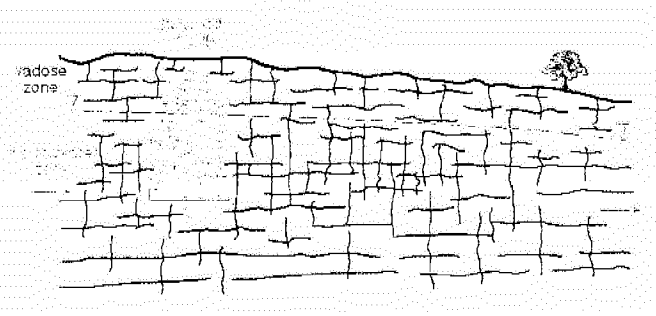

Stage 2: DNAPL Becomes Immobile and Begins to Dissolve

Stage 3: ***Partial DNAPL disappearance and TCE plume development (Figure 6.3).*** In the saturated bedrock, DNAPL began to disappear as it diffused into the rock matrix and its disappearance was accelerated by sorption onto the grains that comprise the rock matrix. The TCE DNAPL disappearance time was influenced strongly by the size of the fracture apertures where it resides, the porosity of the rock matrix, and the fraction of organic carbon, which affects sorption. As the DNAPL disappeared into the rock matrix, it ceased to exist as a continuous interconnected phase and was resident within the fracture network as disconnected segments. DNAPL disappearance is further discussed in section 6.4.

A TCE solute plume developed as the groundwater flowed through the fracture network and TCE was transported by advection. Plume development was retarded by the same processes described above for DNAPL disappearance, but was further attenuated by dispersion within the fracture network. The rate of plume migration was moderate because the concentration gradient between the source and the plume front was fairly high. Timeframes for partial DNAPL disappearance and TCE plume development were expected to range from 10 to 30 years.

Figure 6.3

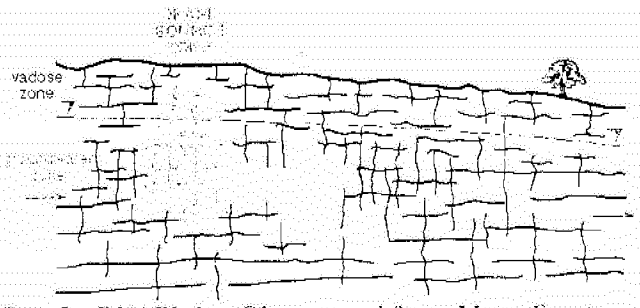

Step 3: DNAPL has Disappeared from Many Fractures and a Dissolved-Phase Plume Develops

HDMSe00012911

Stage 4: ***Complete DNAPL disappearance and TCE plume expansion (Figure 6.4).*** At some point the DNAPL completely disappeared from the fracture network due to diffusion, dissolution and sorption. The timeframes for complete DNAPL disappearance are expected to range from 2 to 50 years due to the variability in fracture apertures and matrix porosity.

The solute plume will continue to expand as the groundwater flows through the fracture network, but the rate of expansion will be very slow because the mass of fractured bedrock available for diffusion greatly increases with plume expansion. The timeframe over which the plume will continue to migrate relative to a concentration limit is expected to range from tens to hundreds of years depending on the duration and mass loading of a DNAPL source.

Figure 6.4

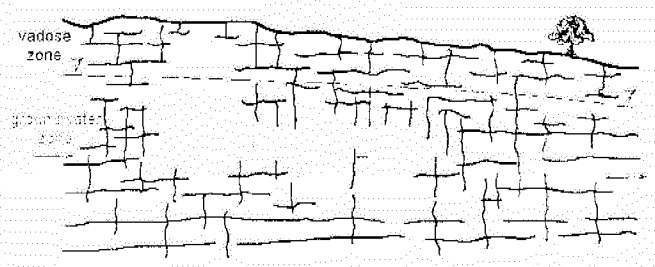

Stage 4: No DNAPL Remains, Plume Has Expanded and Migrates Very Slowly

6.1 DNAPL Flow and Distribution in the Vadose Zone

Four characteristics affect the flow of DNAPL in the Chatsworth Formation vadose zone. These four characteristics are: vadose zone water pressure, water content, fluid wettability and effective permeability. Each of these characteristics and their influence on DNAPL flow is described below. Detailed discussions on the flow and distribution of TCE in the vadose zone are provided in Appendix D.

- **Water Pressure:** By definition, the water pressure within the vadose zone is less than the atmospheric pressure (i.e. negative gage pressure). Negative gage pressures develop in the sandstone matrix because of capillary forces. Water at negative gage pressure preferentially resides in small pore spaces of the bedrock. Smaller and smaller pore spaces will retain water against the force of gravity as the negative gage pressure increases. Since fractures represent the largest openings (or pore spaces) in the rock, they will not be water-filled unless water is available to the fracture at positive gage pressure. Positive gage pressures are likely to arise during infiltration events and below surface water storage ponds. The distribution of water pressure in the vadose zone is shown conceptually in Figure 6.5. Once TCE is released into the bedrock, TCE DNAPL will preferentially and spontaneously flow within the fracture network since the fractures are air-filled except at locations or times noted above.

- **Water Content:** As discussed in section 4.4, the average water content of the vadose zone matrix blocks is determined by the ratio of average recharge flux to the average saturated hydraulic conductivity of the matrix blocks. This ratio is less than unity and represents the mean relative permeability of the sandstone matrix to water. The water content of the matrix adjusts until it is in equilibrium with this ratio. At the SSFL, the mean water content is estimated to be about 0.7 (i.e., the matrix pore space is filled with about 70% water and 30% air, on average). However, the local water content is expected to be highly variable due to variations in rock properties, which is conceptually depicted in Figure 6.5.

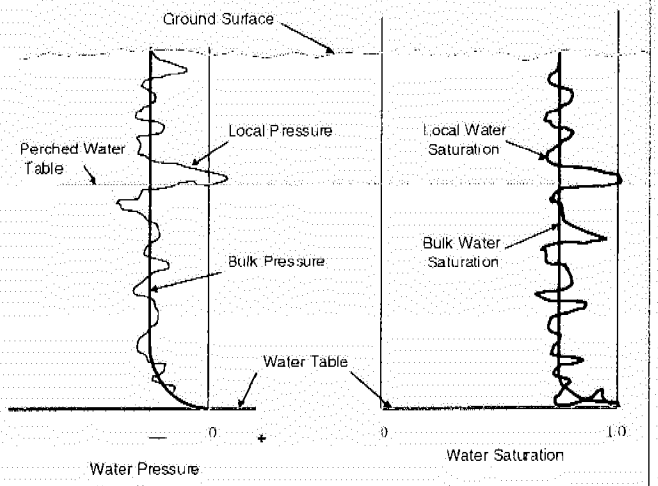

Figure 6.5 Conceptual Distribution of Water Pressure and Content in the Vadose Zone

- **Wettability:** Once DNAPL is released into the bedrock, its distribution and flow will be governed by the wettability of the three fluids (air, water and TCE) resident within the Chatsworth Formation. TCE is the wetting fluid with respect to air. This phenomena will cause the TCE DNAPL within the fractures to be soaked up (or imbibed) into the sandstone matrix adjacent to the walls of the fractures, since the matrix pores contain about 30% air. Imbibition of the TCE, shown conceptually in Figure 6.6, will create a halo of DNAPL around the fractures. TCE DNAPL will not displace the water that is resident within 70% of the sandstone matrix because water is the wetting fluid with respect to TCE.

HDMSe00012912

- **Effective Permeability:** The effective permeability of the matrix to the DNAPL is determined by the intrinsic permeability of the matrix and the pore volume available for DNAPL flow. Since DNAPL can only occupy a small portion of the pores of the rock matrix because of the presence of water and air, the maximum effective permeability of the matrix to DNAPL is a factor of 14 lower than the saturated permeability. Additional calculations show that the reduced permeability limits the penetration of DNAPL into the matrix to only a few centimeters from the fracture wall. The halo of imbibed DNAPL is expected to be quite irregular owing to the local variations in water content. DNAPL imbibition will be prevented at locations where the water content of the matrix is near or at saturation. At these locations, the DNAPL will continue to flow within the fracture network to areas of lower water content and become imbibed, or will flow to the water table. DNAPL is expected to migrate to the water table through the otherwise air-filled fractures within hours to days.

Figure 6.6

Conceptual Distribution of DNAPL in the Vadose Zone

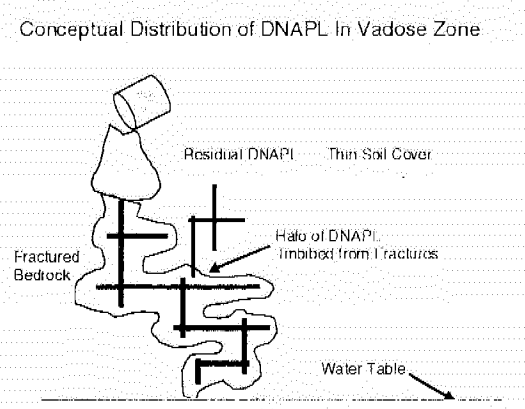

TCE Distribution in the Vadose Zone as a Result of Inter-Phase Partitioning

Inter-phase partitioning (Figure 6.7) will control the distribution of TCE that is imbibed into the sandstone matrix or present within vadose zone fractures. Detailed discussions of inter-phase partitioning in the vadose zone can be found in *Dense Chlorinated Solvents and other DNAPLs in Groundwater* (Pankow and Cherry, 1996). At equilibrium, the inter-phase partitioning includes:

- dissolution of DNAPL into the aqueous phase as characterized by the effective solubility of TCE in water,
- volatilization into the air phase as characterized by the vapor pressure of TCE at the prevailing temperature,
- mass transfer of TCE between the aqueous and gaseous phases, governed by Henry's law and characterized by the dimensionless Henry's constant, and
- sorption of TCE dissolved in the aqueous phase to the solid phase in accordance with the organic carbon partition coefficient and the fraction of organic carbon in the bedrock.

Figure 6.7

Inter-Phase Partitioning of TCE In Unsaturated Matrix Blocks

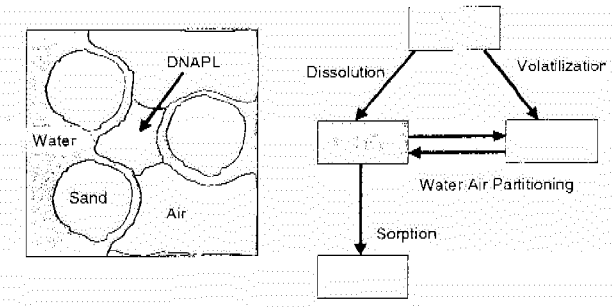

TCE will be distributed by diffusion in all directions from the DNAPL. Its distribution and migration is dominated by gaseous phase diffusion and will produce significant lateral spreading. This is because the gaseous phase diffusion coefficient is approximately 1000 times greater than the aqueous phase diffusion coefficient, even though the air content (which represents the gas) is smaller (30%) than the water content (70%). As TCE spreads in the gaseous phase, it partitions into the aqueous phase. Once in the aqueous phase, TCE is transported primarily downward by advection in the recharge waters. Aqueous phase TCE migration due to advection is affected by partitioning to the rock matrix through sorption.

The result of these mutually-dependent partitioning and transport processes is the creation of a "cloud" of aqueous and gaseous phase TCE around the portion of the fracture system beneath the DNAPL input locations. The lateral spreading that occurs in the vadose zone causes the areal extent of the TCE source zone as observed at the water table to be significantly larger than that observed at the ground surface or at the bedrock contact.

The gaseous phase in the vadose zone is expected to be continuous with atmospheric air, at least through the fractures and possibly through the rock matrix that is not completely saturated with water. These connections provide a pathway for TCE to diffuse to the atmosphere. A substantial portion of the total mass of TCE that has

HDMSe00012913

dissolved from the DNAPL phase may escape to the atmosphere via the ground surface through this process.

TCE Presence and Distribution in Vadose Zone Bedrock at the SSFL

Evidence of the transport of TCE through vadose zone bedrock at the SSFL has been produced from sampling and analysis of rock core at RD-46B. This borehole was placed immediately adjacent to a pond at CTL-III where historic releases of TCE occurred. Analysis of the TCE rock pore water data that were produced from this work reveals that approximately 80% of the mass within the profile occurs within the vadose zone. The variations in concentration with depth in the profile can likely be attributed to variations in the inter-phase partitioning and diffusion that result from variable water content.

6.2 Mass Transfer of TCE Between the Vadose and Groundwater Zones

Recharge waters passing through TCE that has partitioned within the vadose zone transport dissolved TCE to the water table. The transfer of TCE mass from the vadose zone to the groundwater zone was evaluated using an analytical model that accounts for all of the inter-phase partitioning factors described above, except for volatilization of TCE to the atmosphere. The transport processes are shown conceptually below in Figure 6.8.

Figure 6.8

Conceptual Model for Contaminant Transport from Vadose Zone

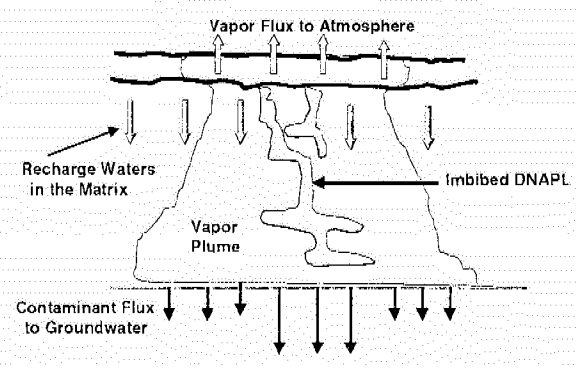

The results of these numerical simulations reveal the following:

- The dissolution rate of TCE from the vadose zone to the saturated zone is expected to be fairly small, in the range of a few tenths of a kilogram to a few kilograms per year and depends upon the areal extent of the cloud of TCE in the vadose zone. The assumed conditions for these calculations included a recharge rate that was varied from 1 inch per year to 4 inches per year. The dimension of the zone of imbibed DNAPL were 0.5 meters wide by 10 meters high by an infinite length.

- The concentration of TCE in the recharge waters is greatest below areas where DNAPL has become imbibed within the matrix. The mass flux is also highest here because the aqueous concentrations of TCE are high.

- The mass discharge from the footprint of the vapor plume dominates the overall mass discharge to groundwater because the areal extent of the vapor plume is much greater than the areal extent of the imbibed TCE, even though the mass flux is significantly lower.

- The dissolution rate of TCE from the vadose zone to the groundwater decreases as the groundwater recharge rate increases.

- Varying the number of parallel fractures and the fracture spacing indicates that the vadose zone TCE dissolution rate is moderately sensitive to these parameters (by factors of between 2 and 4).

6.3 DNAPL Flow and Distribution in the Saturated Zone

The flow and distribution of DNAPL in the saturated zone, shown conceptually in Figure 6.9, is controlled by entry and fluid pressures.

Figure 6.9

Conceptual Distribution of DNAPL Below the Water Table During DNAPL Entry Into the Saturated Zone

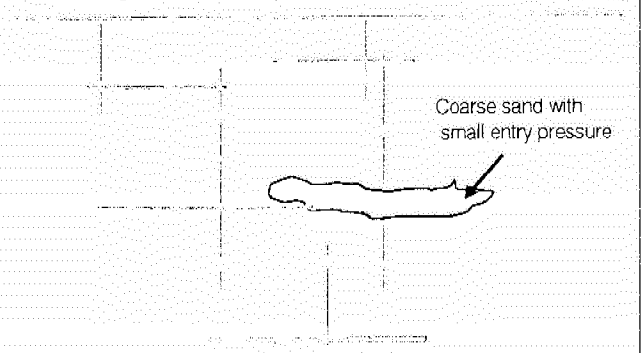

HDMSe00012914

By definition, water pressures in the saturated zone are positive. Therefore, all interconnected openings, both fracture and rock matrix, are water-filled below the water table. Since TCE DNAPL is the non-wetting fluid with respect to water, it requires positive pressure to enter any water-filled openings.

DNAPL will enter a water-filled opening only if its pressure exceeds the water pressure by some threshold value. This threshold is called the entry capillary pressure or simply the entry pressure. The entry pressure is dependent upon the:

- interfacial tension between liquid-phase TCE and water,
- contact angle, and
- size of the opening across which the two-fluid interface is positioned.

Entry pressures generally increase as the size of the opening across the two-fluid interface decreases, assuming that the geometry, interfacial tension and fluid wettability remain constant.

The entry pressure of the fracture system at the SSFL is much smaller than matrix block entry pressures since fracture openings are much larger than openings in the matrix. DNAPL is expected to migrate and reside primarily in fractures below the water table. Once the DNAPL source is exhausted, DNAPL in the fracture system drains. However, drainage is not complete, and a residual remains after the fracture drains (Figure 6.10). The formation of the trail of residual consumes the mobile DNAPL and limits the depth of DNAPL migration.

Figure 6.10

Redistribution of DNAPL Below the Water Table After a Release Has Ceased

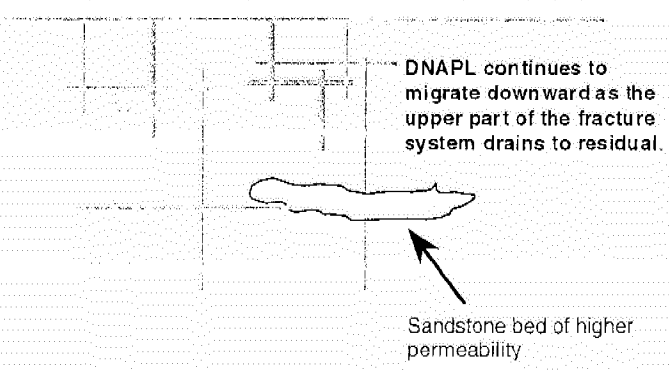

The depth of DNAPL penetration below the water table is also effected by a number of physical characteristics at the site

- **The presence of strong local upward hydraulic gradients.** Local upward gradients can be large, even when the average upward gradient indicated by piezometer measurements is small as shown in Figure 6.11. Strong local upward gradients were present at RD-46 as shown by groundwater monitoring results using a multi-level monitoring device.

Figure 6.11

Local Hydraulic Gradient May Be Large, Even When Average Is Modest

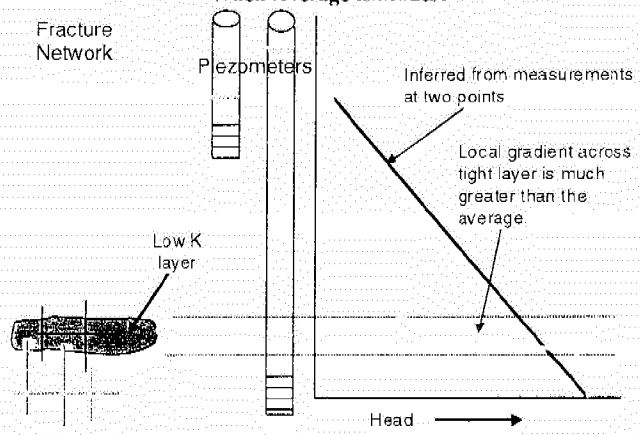

- **Entry and retention of the TCE DNAPL within coarse sandstone beds where entry pressures are lower.** Entry pressures are reduced within coarse sandstone beds due to an increase in the pore space openings. These increased pore space openings result in increased hydraulic conductivity. TCE rock pore water results indicate that coarse sandstone beds likely present a significant area for TCE storage.

- **Partitioning and retention of the TCE DNAPL within the vadose zone.** As presented in section 6.1, TCE DNAPL partitions into and becomes retained within the vadose zone as solute and vapor.

- **Retention of the TCE DNAPL within fractures.** The porosity of the fracture system provides storage capacity for DNAPL within the fracture network.

- **Increasing entry pressures with depth due to lithostatic loading.** Lithostatic loading likely results in smaller fracture apertures with increasing depth.

- **Loss of DNAPL mass due to matrix diffusion.** DNAPL dissolves into the rock matrix through diffusion and loses it mass resulting in disconnected segments of DNAPL. These effects are more fully discussed in the following section.

HDMSe00012915

- Shunting of DNAPL flow through vertical fractures by bedding plane fractures. A discussion was presented in section 3.5 stating that the vertical fractures at the SSFL are typically confined within single sandstone beds, where they terminate at the bedding plane. These points-of-termination force the DNAPL to flow along the bedding plane and shunt its vertical penetration.

- The presence of shale or other low permeability beds. These features limit DNAPL penetration because the fracture apertures within the beds are significantly smaller than within the sandstone, thus increasing the entry pressure.

6.4 Effects of Matrix Diffusion on TCE DNAPL Below the Water Table

Once DNAPL is present in the fracture network below the water table, it diffuses into the sandstone matrix according to Fick's Law and dissolves in the groundwater as controlled by its aqueous solubility. This process is conceptually shown on Figure 6.12. Detailed descriptions of this process are provided in section 3.0 of Appendix E.

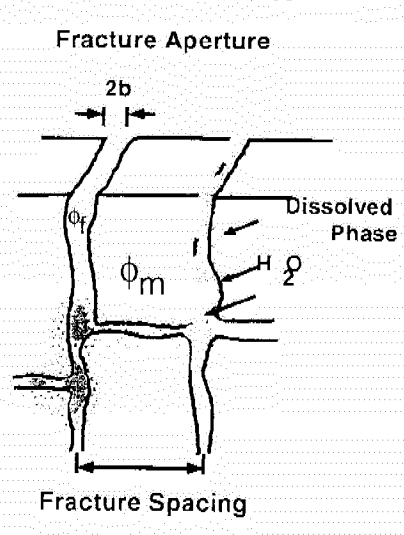

Figure 6.12 Conceptual diagram of TCE DNAPL dissolving away from fractures and into the sandstone matrix.

DNAPL disappearance through matrix diffusion in fractured bedrock results when the mass storage capacity of the rock matrix exceeds the mass storage capacity of the fracture network (Figure 6.13). Calculations were made using Chatsworth Formation data to estimate the ratio of the matrix storage capacity to the fracture storage capacity.

These results showed that the Chatsworth Formation sandstone can store between 5 and 100 times the mass of DNAPL within the matrix than within the fracture and that DNAPL disappearance through matrix diffusion is expected.

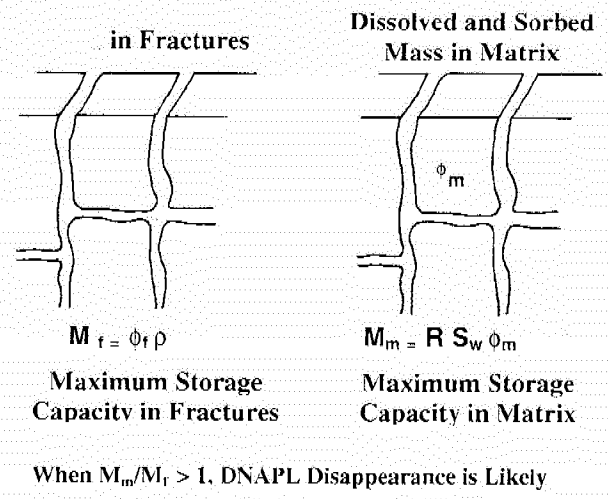

Figure 6.13 DNAPL mass storage capacities in fracture network and matrix

The effect that matrix diffusion has on DNAPL dissolution can be quantified using a solution to Fick's second law. The time for DNAPL to disappear from Chatsworth Formation fractures can be calculated by solving Fick's second law and results in the following equation for a single parallel-plate fracture:

$$t_D = \frac{\pi \rho^2 (2b)^2}{16 S_w \phi_m^2 D_e R_m}$$

where:

t_D = DNAPL disappearance time
ρ = density of TCE
$2b$ = fracture aperture
S_w = aqueous solubility of TCE
ϕ_m = matrix porosity
D_e = diffusion coefficient
R_m = retardation in the matrix due to sorption, calculated by

$$R_m = 1 + (\rho_b/\phi_m)(K_{oc} \times f_{oc})$$

where:

ρ_b = dry bulk density
ϕ_m = matrix porosity
K_{oc} = octanol-water partition coefficient for TCE
f_{oc} = fraction of organic carbon

HDMSe00012916

Site-specific data were used to quantify average values for matrix porosity, the diffusion coefficient and organic carbon. Values are shown on Table 6.1. DNAPL disappearance times were calculated using these average values along with estimates of the size of fracture apertures that were determined from pumping tests and advanced downhole geophysical tests at RD-35B and RD-46B. The calculations show that matrix diffusion causes DNAPL to disappear from fractures in timeframes ranging from 2 to 50 years.

Property	*No. of Measurements*	*Minimum*	*Maximum*	*Mean*
Porosity (%)	59	1.0	21.60	12.86
Diffusion Coefficient (cm^2/sec)	10	7.5×10^{-7}	2.2×10^{-6}	1.5×10^{-6}
Fraction Organic Carbon (%)	8	0.02	0.15	0.10
Hydraulic Fracture Apertures (microns)	Not applicable	10	300	100

Table 6.1 Values of Input Parameters for DNAPL Disappearance Calculations

These DNAPL disappearance calculations do not consider the additive effect on DNAPL dissolution that results from bulk groundwater flow (advection). DNAPL dissolution associated with groundwater flow through the fracture network was qualitatively evaluated through the use of a fate and transport model that was developed for fractured porous media (VanderKwaak and Sudicky, 1996). Simulations were made using the model to quantify DNAPL disappearance times associated with matrix diffusion with and without the effects of advection. The simulation results for a single fracture having an aperture of 100 microns showed a reduction in the DNAPL disappearance times from 5.4 years without advection to 0.16 years with advection, which is about 30 times shorter. It is expected that a similar reduction in the DNAPL disappearance times that were calculated for RD-35B and RD-46B (where advection was not included) would result.

Site-Specific Data Indicating the Disappearance of DNAPL

Two boreholes (RD-35B and RD-46B) were the focus of intensive studies to determine the effects of matrix diffusion on TCE in Chatsworth Formation groundwater (Sterling, 1999). These boreholes were located immediately adjacent to or near suspected TCE input locations. As mentioned in section 6.1, RD-46B was located adjacent to a pond at CTL-III and RD-35B was located near suspected sources at IEL where TCE concentrations in groundwater were high (in the tens of mg/L range). Over 277 samples of rock core were collected and analyzed for the presence and concentration of VOCs from these two locations. One hundred twelve (112) of the 277 samples contained TCE above the method detection limit of about 0.5 mg/L (See Figure 6.14). The highest concentration of TCE detected in the rock pore water from either location was 164 mg/L. This value is approximately one order-of-magnitude lower than the aqueous solubility of TCE (1420 mg/L) and provides supporting evidence that almost all of the DNAPL that may have entered the Chatsworth Formation groundwater has disappeared.

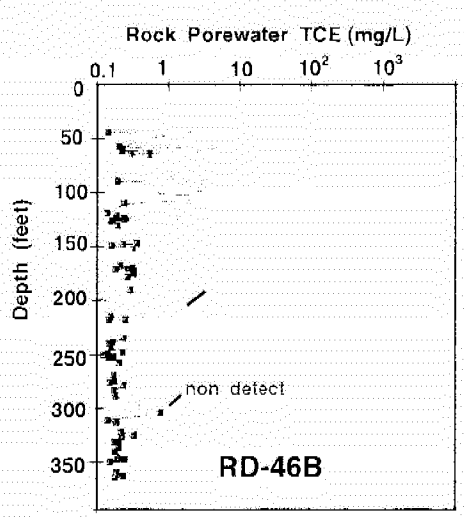

Figure 6.14

Results of rock core analyses from RD-35B and RD-46B. Maximum concentrations detected are one order-of-magnitude below the aqueous solubility.

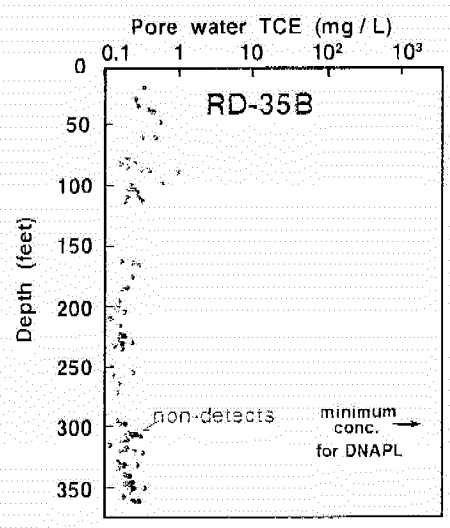

HDMSe00012917

6.5 Summary of Flow, Distribution and Fate of TCE DNAPL in Source Zones

TCE as a DNAPL flowed through the fractures in the vadose zone bedrock and spontaneously imbibed into the matrix a distance of a few centimeters. Once in the matrix, TCE partitioned into the gaseous and aqueous phases and sorbed onto the matrix grains from the aqueous phase. TCE was transported to the ground surface in the gaseous phase and volatilized to the atmosphere or was transported to the groundwater by advection in the flowing recharge waters. Dissolution rates from the vadose zone to the groundwater zone at source areas are expected to be fairly small (few tenths of a kilogram to a few kilograms per year).

TCE DNAPL that is transported through the vadose zone and to the saturated zone must establish a certain head to overcome the relatively small entry pressures of the fractures to penetrate below the water table. The migration of TCE into the fracture network can be stopped due to a number of processes. Once TCE is within the fracture network, the DNAPL begins to dissolve due to molecular diffusion into the sandstone matrix, sorption onto the matrix grains and dissolution into the groundwater flowing in the fracture network. DNAPL is expected to be present in the Chatsworth Formation fracture network for periods ranging from 2 to 50 years.

HDMSe00012918

7.0 Transport and Fate of TCE Solute

The porous sandstone matrix of the Chatsworth Formation has a strong influence on the migration rate of dissolved-phase TCE flowing through the fracture network. This section of the technical memorandum describes and quantifies the effects that matrix diffusion and sorption have on migration rates of the TCE solute. Additional descriptions and supporting documentation are provided in Appendices E and F. The retardation process is shown conceptually in Figure 7.1.

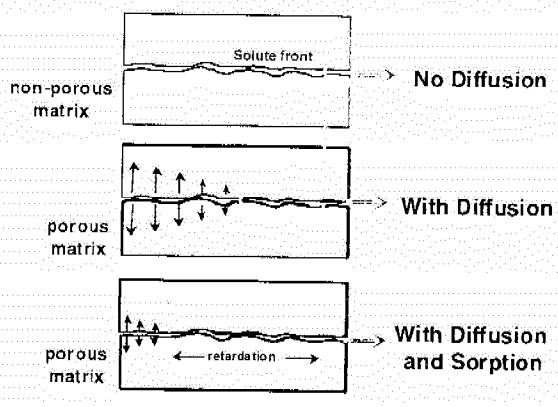

Figure 7.1 Conceptual Effect of Retardation of TCE due to Matrix Diffusion and Sorption

The approaches taken to assess the migration rates of the TCE solute include:

- Applying a numerical model (FRACTRAN, Sudicky and McLaren, 1992) to simulate groundwater flow and TCE transport a single fracture, and to evaluate and quantify the retardation effects of matrix diffusion on TCE migration. A full description and details of the modeling are provided in Appendix F. The numerical model is also used to evaluate the sensitivity of migration rates to changes in geologic and hydrogeologic properties including:

  - ✓ matrix porosity,
  - ✓ retardation in the matrix due to sorption,
  - ✓ the diffusion coefficient,
  - ✓ hydraulic conductivity,
  - ✓ fracture apertures, and
  - ✓ hydraulic gradient.

  The timeframe over which a DNAPL source is present is also varied to assess the effect on TCE plume migration rates. Varying the duration of the DNAPL source reflects the expectation that DNAPL dissolves away from the fracture network due to matrix diffusion and advection as was discussed in section 6.4.

- Applying FRACTRAN to a two-dimensional fracture network that more closely simulates migration of TCE solute through the Chatsworth Formation. The two-dimensional model is also used to predict plume characteristics and to demonstrate the effects of retardation in an interconnected fracture network.

- Comparing model results to field data to assess the current stage of plume migration at the SSFL.

The evaluation of the retardation rates of the TCE solute is presented in the context of the average linear groundwater velocity in a fracture network. As presented in section 4.9, the average linear groundwater velocity at SSFL is expected to range from 500 to 10,000 feet per year. Actual groundwater velocities will be faster than the calculated average linear velocity due to the tortuous pathway in the fracture network through which the groundwater must travel. Diffusion of the TCE solute into the sandstone matrix is expected to cause TCE to migrate at rates much slower than the average linear groundwater velocity.

Definitions

The time required for the front of a TCE plume to migrate a specific distance downgradient can be compared to the time for groundwater to travel the same distance. The comparison of the TCE arrival time to the groundwater arrival time is defined as the "**apparent retardation**". The plume front can be defined as the ratio of a specific concentration "C" (e.g., 1.42 mg/L) relative to a source concentration C_0 (e.g., 1420 mg/L, the aqueous solubility of TCE). In this example, the ratio, $\mathbf{C/C_0}$, is equal to 1.42/1420, or 1×10^{-3}. Further discussions on the TCE solute migration will frequently reference these two terms.

7.1 TCE Solute Transport and Retardation in a Single Fracture

Two different model domains were established for the single-fracture simulations on the transport of TCE solute. A model domain of 5 meters (m) in the vertical dimension (or "z") by 200 m in the horizontal dimension (or "x") was established for the initial simulations (Figure 7.2). Input parameters for the initial simulation (i.e., the base case) included the following:

- matrix porosity, $\phi_m = 10\%$
- retardation factor associated with sorption, $R_m = 1.0$
- diffusion coefficient, $D_e = 10^{-6}$ cm^2/sec
- hydraulic gradient, i = 1%
- fracture aperture, 2b = 100 μm

HDMSe00012919

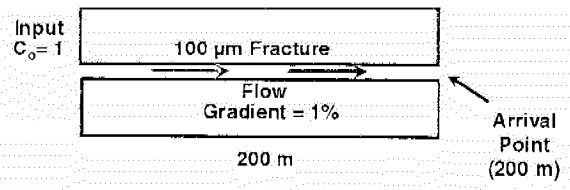

Model Domain Single Fracture Simulations

Figure 7.2

The objective of these simulations was to evaluate the effects of matrix diffusion on the migration of the TCE solute by quantifying the time of arrival for the TCE plume front relative to the groundwater arrival time at a C/C_0 of 10^{-3}. A constant source input function representing TCE DNAPL was placed at the upgradient boundary of the model at x = 0 m. This model was also used to quantify the effects that variations of the input parameters have on the arrival time of the TCE plume front relative to the base case. Results are presented in Table 7.1.

	Parameter Value	*Arrival Time at 200 m*	*Apparent Retardation*
roundwater	NA	28 days	1
CE Solute Sorption	$R_m = 1$	4 yrs. (Base Case)	52
	$R_m = 3$	11.5 yrs.	150
Porosity (%)	5	1.6 yrs.	21
	10	4.0 yrs. (Base Case)	52
	15	8.6 yrs.	112
Diffusion Coefficient (cm^2/sec)	1×10^{-6}	4.0 yrs. (Base Case)	52
	2×10^{-6}	7.5 yrs.	98
Fracture Aperture (µm)	100	4.0 yrs. (Base Case)	52
	200	0.2 yrs.	3

Table 7.1 This table summarizes the affects that changing parameters have on the apparent retardation of the TCE plume front at a C/C_0 of 10^{-3}. Other parameters shown in the base case are held constant while each individual parameter is varied to determine its affect on the arrival time.

In summary, the simulations show that matrix diffusion causes TCE to arrive at a distance 200 m downgradient of the DNAPL input location, which also represents the end of the model domain, in 4 years, while groundwater arrives at this same location in 28 days. Comparing the TCE arrival time to the groundwater arrival time results in an apparent retardation factor of 52 for the base case. When the base case is altered to include sorption, TCE arrives at the end of the model domain in 11.5 years. These simulations show the strong retardation effect that matrix diffusion has on the migration of TCE solute along a single fracture.

The same model domain was used to evaluate the effects on the arrival time of the TCE solute that result from varying the relative concentration or C/C_0. These simulations were also used to evaluate what changes hydraulic gradient has on the arrival time of TCE solute. The input parameters for this second set of simulations (base case) were changed to be more representative of the Chatsworth Formation and were as follows:

- matrix porosity, $\phi_m = 13\%$
- retardation factor associated with sorption, $R_m = 3.0$
- diffusion coefficient, $D_e = 10^{-6}$ cm^2/sec
- hydraulic gradient, i = 2%
- fracture aperture, 2b = 70 µm

Results from these simulations show that it takes longer for the TCE plume front to arrive as the C/C_0 increases (i.e., the higher concentration portions of the plume arrive at a specified location at a much later time than the lower concentration portions of the plume). The results also show that the apparent retardation factor increases as the distance from the source input increases. This decreasing rate-of-change or deceleration of plume front arrival is the result of the plume invading an ever-increasing volume of Chatsworth Formation sandstone, which provides increased TCE storage capacity. Decreasing the hydraulic gradient from 2% to 1% results in a reduction in the arrival time of the TCE plume front at the end of the model domain by a factor of about 4, from 21 years to 86 years.

A slightly larger model domain of the single fracture case was used to evaluate the effects on arrival time of the TCE solute that result from varying the timeframe over which a DNAPL source is present. This larger model domain was also used to evaluate what changes in TCE concentrations within the plume would result after very long periods of time (e.g., 500 years) when the source has a finite life. The model domain used in these simulations was expanded to 10 m in the z-direction and to 500 m in the x-direction. Input parameters to the model were as follows:

- matrix porosity, $\phi_m = 13\%$
- retardation factor associated with sorption, $R_m = 3.0$
- diffusion coefficient, $D_e = 10^{-6}$ cm^2/sec
- hydraulic gradient, i = 1%
- fracture aperture, 2b = 70 µm

Simulations were made using two types of sources:

HDMSe00012920

- A constant source throughout the entire simulation to represent persistent DNAPL, and

- A 10-year finite term to represent DNAPL dissolution. Although the DNAPL phase has disappeared, the TCE mass from the DNAPL remains in the source area for a long time continuing to contribute mass to the plume, but at diminishing concentrations.

The 10-year finite case is believed to more accurately reflect conditions at the SSFL where TCE DNAPL disappears due to matrix diffusion and advective dissolution.

The simulation results show that the maximum concentrations of TCE solute in the plume are greatly reduced when a source of TCE DNAPL is present over a finite period. This effect is graphically presented on Figure 7.3.

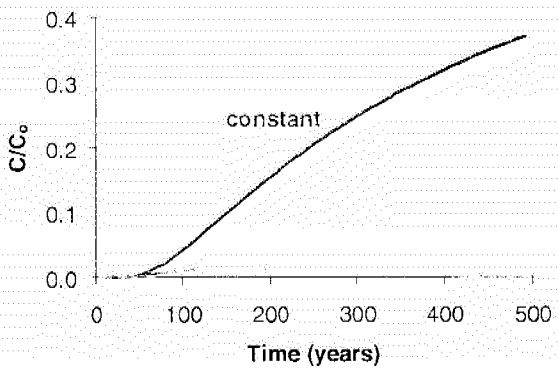

Figure 7.3 Graph of relative TCE concentrations over time for constant and 10-year sources at x=200 m. Concentrations in the constant source condition continually increase while the concentrations in the 10-year source condition peak and then gradually decrease. The maximum concentration in the 10-year source condition is also much lower than the constant source condition.

The model results also show that TCE concentrations within the plume naturally attenuate or reduce over time. After several decades, the plume front is essentially stable as its rate of migration has slowed to less than 2 m/year and will continue to migrate at ever-decreasing rates relative to a defined concentration. This effect on plume migration is shown on Figure 7.4

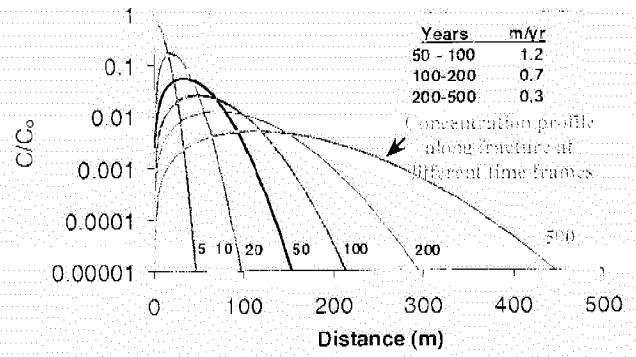

Figure 7.4 Relative TCE concentration profiles along the fracture under the 10-year source condition. Migration rates of the plume front at a C/C_o of 10^{-5} are also shown for three different time frames.

The results of the simulations presented in this section show the ultimate effects of matrix diffusion and sorption on the fate of TCE. The eventual dissolution of the DNAPL phase indicates the end of the source condition as solute-free groundwater from upgradient of the source zone begins to flush the fractures and reverse the concentration gradient causing diffusion from the matrix blocks back into the fractures (reverse diffusion). The process of reverse diffusion is shown conceptually in Figure 7.5.

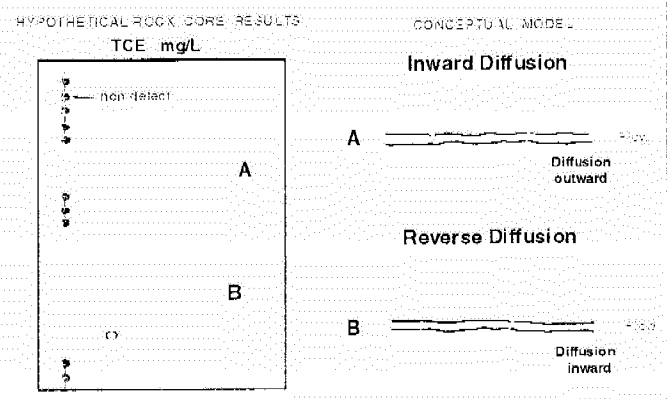

Figure 7.5 Conceptual depiction of diffusion from the matrix bedrock into the groundwater flowing through the fractures (shown as condition 'B'). Note the change in the concentration profile in the hypothetical rock core results. As groundwater passes through the fractures, the pore water concentration in the matrix adjacent to the fracture decrease first, while those deeper into the matrix remain elevated.

HDMSe00012921

The process of flushing the source zone is initiated as the mass is transported downgradient in a much more dilute form, which is also susceptible to matrix diffusion and sorption as it migrates in the plume. This concept gives rise to a fifth stage of the TCE plume development, the first four of which were presented in section 6.0. This stage is characterized as follows:

- Stage 5: *Source Zone is Clean and Plume Front is Stable or Retreating (Figure 7.6)*. Groundwater at the original source zone where DNAPL was present no longer contains concentrations exceeding a threshold value. The continually diminishing concentrations in the plume cause the rate of migration of the TCE solute at the plume front to slow considerably or stop. As lower and lower concentrations of TCE continue to diffuse out of the matrix blocks into the clean groundwater flowing in the fracture network from upgradient, the plume will appear to retreat by moving upgradient relative to a defined concentration value (e.g., 0.005 mg/L). Eventually all areas of the former source zone and plume will contain concentrations of TCE below a defined concentration limit.

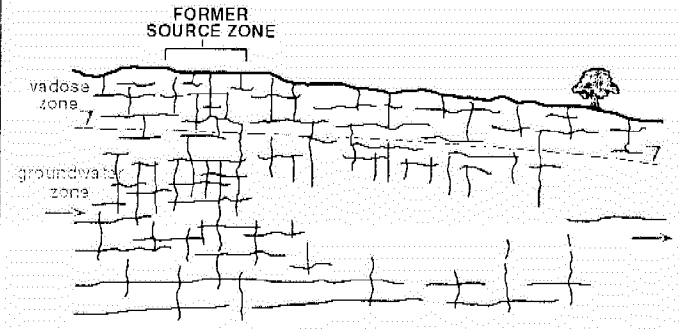

Figure 7.6

Stage 5 Source Zone is Clean and Plume Front is Stable or Retreating

7.2 TCE Solute Transport and Retardation in a Two-Dimensional Fracture Network

The same numerical model was used to simulate the migration of TCE solute in a two-dimensional fracture network. The objective of these simulations was to develop an understanding of the transport and fate of TCE over long periods of time (e.g. 500 years) in an interconnected fracture network of sandstone while using input parameters similar to the Chatsworth Formation. Model properties and input parameters were as follows:

- orthogonal fracture network with variable fracture apertures shown in Figure 7-7, mean aperture, 2b = 70 μm, minimum aperture less than 30 μm and maximum aperture of greater than 250 μm.
- retardation factor associated with sorption, $R_m = 3.0$
- steady state groundwater flow,
- source constant for 10 years at TCE solubility,
- matrix porosity, $\phi_m = 13\%$
- hydraulic gradient,
  - ✓ horizontal 2%,
  - ✓ vertical = 1%
- diffusion coefficient, $D_e = 10^{-6}$ cm²/sec,
- bulk hydraulic conductivity,
  - ✓ horizontal: $K_x = 1.5 \times 10^{-5}$ cm/sec
  - ✓ vertical: $K_z = 3.0 \times 10^{-6}$ cm/sec (anisotropy ratio of ~5)
- fracture porosity, $\phi_f = 5.9 \times 10^{-5}$
- average linear groundwater velocity, v_l = 1.6 km/yr (1 mile per year)

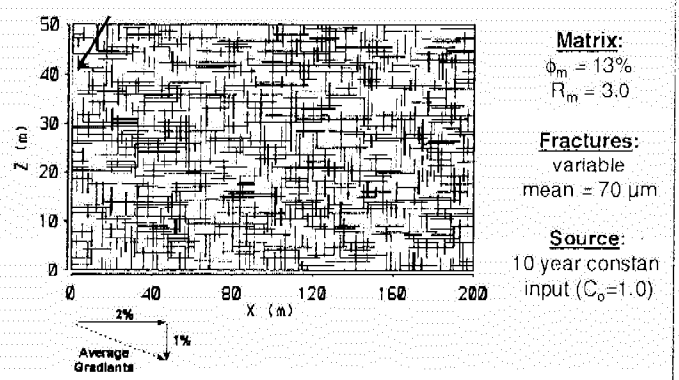

Figure 7.7 Variable aperture network used for two-dimensional vertical simulation of TCE transport.

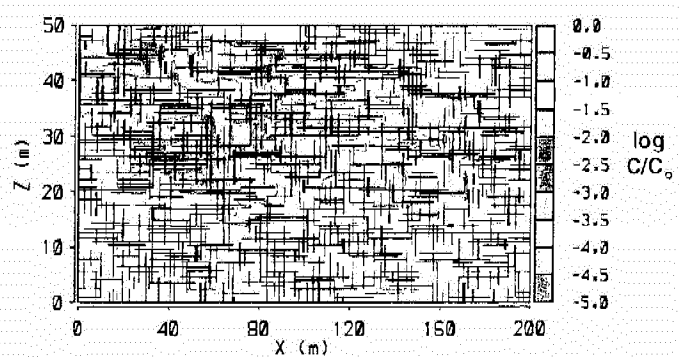

Figure 7.8 TCE plume at 50 years

Simulations were performed for durations extending to 500 years. The graphic output of the model results of the TCE plume at 50 years is shown on Figure 7.8.

HDMSe00012922

Results of the simulations were consistent with those of the single-fracture simulations and revealed the following:

- The maximum concentration of TCE in the plume decreases over time as shown on Table 7.1.

Time (years)	Maximum Relative Concentration in Plume (C/C_o)
20	0.66
50	0.51
100	0.2
500	0.03

Table 7.1 Changes in the maximum relative concentration over time from the two-dimensional modeling simulation.

- The time of arrival of the plume front becomes longer as the distance from the source input increases. Arrival times for fractures containing the highest concentrations of TCE were 1.1, 5.9 and 16 years at distances of 50 m, 100 m and 200 m from the source, respectively. The increasing time of arrival with distances is shown on Figure 7.9.

Figure 7.9 TCE arrival over time for the highest

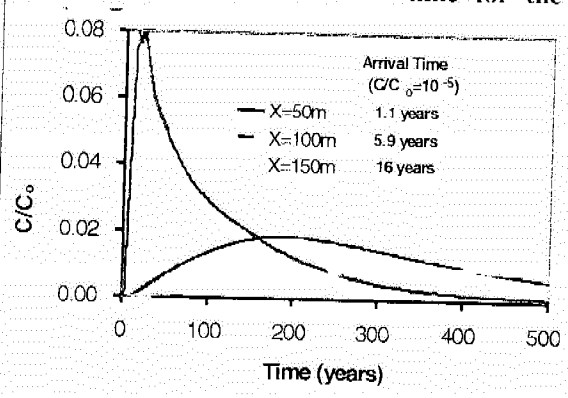

concentration fracture in the network at a distance of 50m, 100m and 150m from the source. Note that the time when TCE first arrives at each of these locations increases with distance from the source. Note also the shape of the concentration curve at each location where concentration increases, peaks and slowly decreases.

- The concentration at a specified distance from the source decreases over time. As an example, the relative concentration in the fracture containing the highest concentration of TCE at a location 100 m from the source over time is summarized in Table 7.2

Time (years)	Maximum Relative Concentration (C/C_o) at x = 100m
100	0.014
200	0.018
300	0.015
400	0.01
500	0.006

Table 7.2 Changes in the relative concentration of TCE over time in the highest concentration fracture at x = 100m

- The area where the TCE source was located no longer contains concentrations above a C/C_0 of 10^{-5} within 500 years indicating the source and plume will naturally attenuate. The results also show that approximately 75% of the mass that entered the system during the 10-year source period remains within the 200 meter model domain after 500 years, which provides supporting evidence that the mass of TCE remains near the input location.

7.3 Comparison of Model Results with Field Data

Vertical TCE concentration profiles are one of the output files that are produced from the modeling simulations. Vertical profiles produced from the simulations were compared to the vertical profiles produced from sampling and analysis of the rock core from RD-35B and RD-46B. These comparisons were made to qualitatively assess whether the model forecasts conditions similar to those observed in the field. Comparison of the vertical TCE profiles from the model with those from the field shows the profiles to be similar in their shape and peak concentrations, as shown on Figure 7.10.

HDMSe00012923

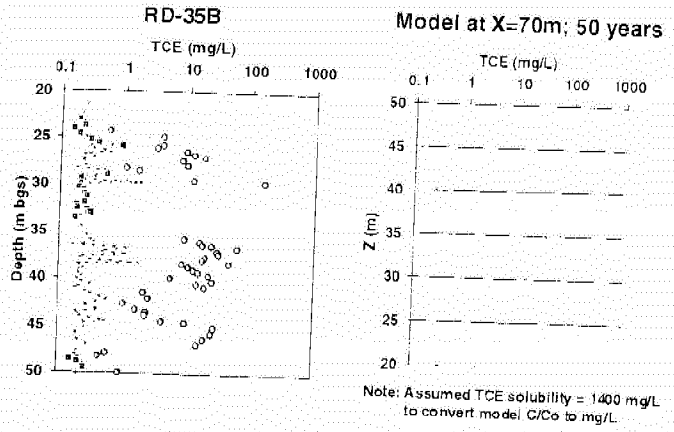

Figure 7.10 Rock core results from RD-35B are compared to hypothetical rock core results from the modeling simulations at a projected distance and time believed to be representative of the conditions at RD-35B. The shape and peak concentrations of TCE in rock pore water between field data and model output are similar.

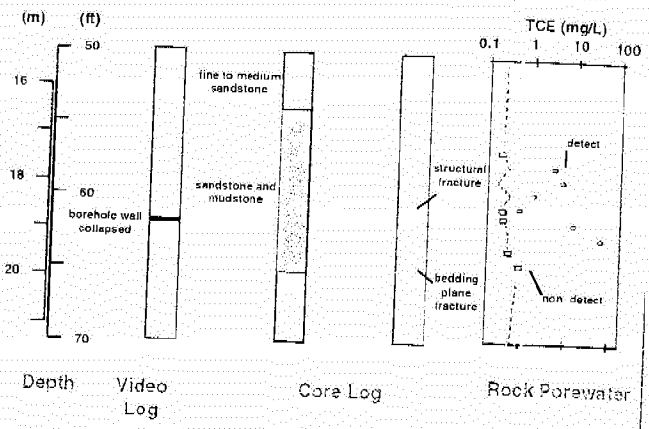

Figure 7.11 Fracture and TCE rock pore water data from RD-46B. Note that the TCE concentrations in rock core immediately adjacent to the fracture are lower than the concentrations deeper into the matrix. These conditions, which were conceptually presented in Figure 7.5, indicate that TCE is diffusing from the matrix into the groundwater flowing through the fractures and are indicative of stage 4 of plume evolution.

The rock core results from RD-35B and RD-46B were inspected to determine the current stage of plume migration in Chatsworth Formation groundwater. Inspection of the vertical TCE profiles and fractures at RD-46B indicates that the matrix is releasing TCE back into the groundwater flowing within the fracture network. Rock core concentrations and fracture locations from the core log are shown on Figure 7.11. This "reverse diffusion" process occurs when the concentration gradient between groundwater retained within the sandstone matrix and the groundwater flowing through the fractures is reversed (i.e. water flowing through the fracture network is cleaner than the pore water within the sandstone matrix blocks).

Reverse diffusion is characteristic of stage 4 of plume development when no DNAPL remains in the fracture network and plume migration is very slow. Calculations were made using an analytical solution to Fick's second law to evaluate the rate of TCE mass removal from the matrix blocks to groundwater flowing through the fracture network (Parker, McWhorter and Cherry, 1997). A graph of the mass removal rate of TCE from tabular matrix blocks is presented on Figure 7.12. As can be seen from the graph, the rate of diffusion out of the matrix is very slow and the mass removal rate becomes asymptotic with time. This indicates that long time frames are needed for reverse matrix diffusion to transfer the TCE back out of the matrix.

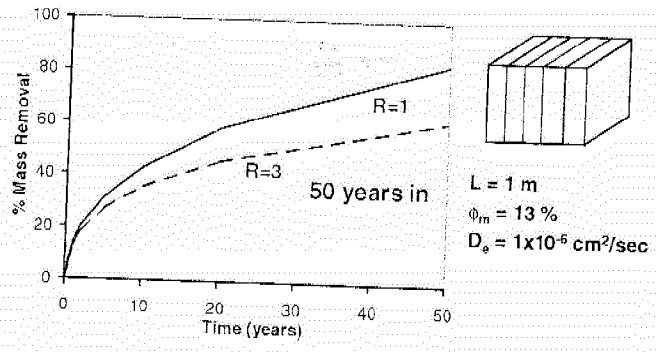

Figure 7.12 Graph of TCE mass removal from tabular matrix blocks over time. Mass removal rates are plotted for two finite-term source conditions, 5 and 50 years. The effects of sorption on the rate of mass removal through reverse diffusion are also plotted on the figure. Note that under the 5 year source condition that approximately 20% of the mass remains in the matrix blocks after 50 years of flushing.

HDMSe00012924

7.4 Summary

Diffusion, sorption and dispersion of TCE solute into the sandstone matrix of the Chatsworth Formation cause the rate of migration of TCE to be orders of magnitude lower than the average linear groundwater velocity within distances of hundreds of feet from the source zone. The rate of migration is very slow (<2 m/yr) or nearly stationary within decades after releases have stopped. Elevated concentrations remain near the input locations. The concentrations in the source zone and plume continue to decline over time (hundreds of years) as mass is transferred back out of the matrix and into groundwater flowing through the fracture network. Rock core data indicates that the plumes at the SSFL are likely in Stage 4. The stages of plume front advancement are conceptually shown on Figure 7.13.

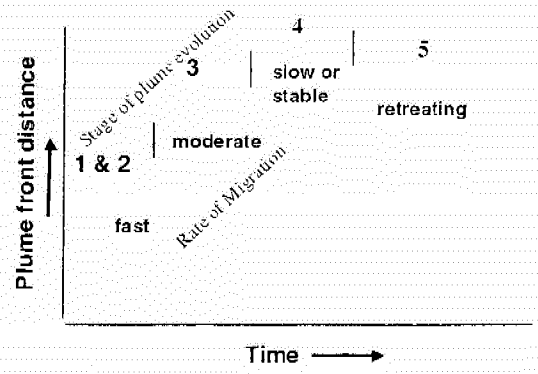

Figure 7.13 Graph of conceptual migration rates of each plume stage over time and distance.

HDMSe00012925

8.0 Monitoring Chatsworth Formation Groundwater

Three characteristics of the Chatsworth Formation are believed to distribute TCE throughout the groundwater system in an orderly and predictable manner. These characteristics produce plumes that can be detected, characterized and monitored and include:

- An interconnected fracture network,
- Strong retardation of the plume as a result of matrix diffusion and sorption and,
- Distributory influence of dispersion on solute behavior.

Additional descriptions on the applicability of groundwater monitoring are provided in Appendix G.

8.1 Interconnected Fracture Network

Several different lines of evidence of an interconnected fracture network were previously presented in section 4.7. Additional information on the interconnected fracture network of the Chatsworth Formation has been developed from the sampling and analysis of rock core. All data that were collected during the rock coring program were reviewed to determine whether the TCE identified in the rock core was associated with transport of the TCE through the fracture network or through sandstone beds having higher permeability due to coarser grain sizes. Data that were assimilated to make this determination included: inspection and description of the rock core to identify fractures, advanced downhole geophysical methods that provided data as to whether fractures were open, their orientation and groundwater flow characteristics (rate and direction) within fracture zones.

In summary, as shown in Figure 8.1, these data show th transport of TCE in many fractures in both boreholes, alon with transport through a number of more permeabl sandstone beds. TCE transport through many fracture indicates that the fracture network is interconnected.

8.2 Plume Retardation

The effects that matrix diffusion and sorption have on retarding the migration rate of TCE solute relative to the average linear groundwater velocity were presented in section 7.0 and are fully discussed in Appendix E. Strong retardation primarily effects the ability to monitor the groundwater because the highest concentrations remain near the input location and the plume front will have migrated only short distances from the input location relative to the average linear groundwater velocity. The large capacity of the rock matrix to store TCE results in the broad, three-dimensional distribution of TCE solute within the fracture network as well as within the rock matrix as shown in Figure 8.2. The large spatial distribution results in a "plume" of TCE that can be located, characterized and, if necessary, delineated. Placement of an appropriately designed monitoring device within the "plume" would provide useful and reproducible information as to the presence and concentration of TCE solute migrating at any location within the fracture network.

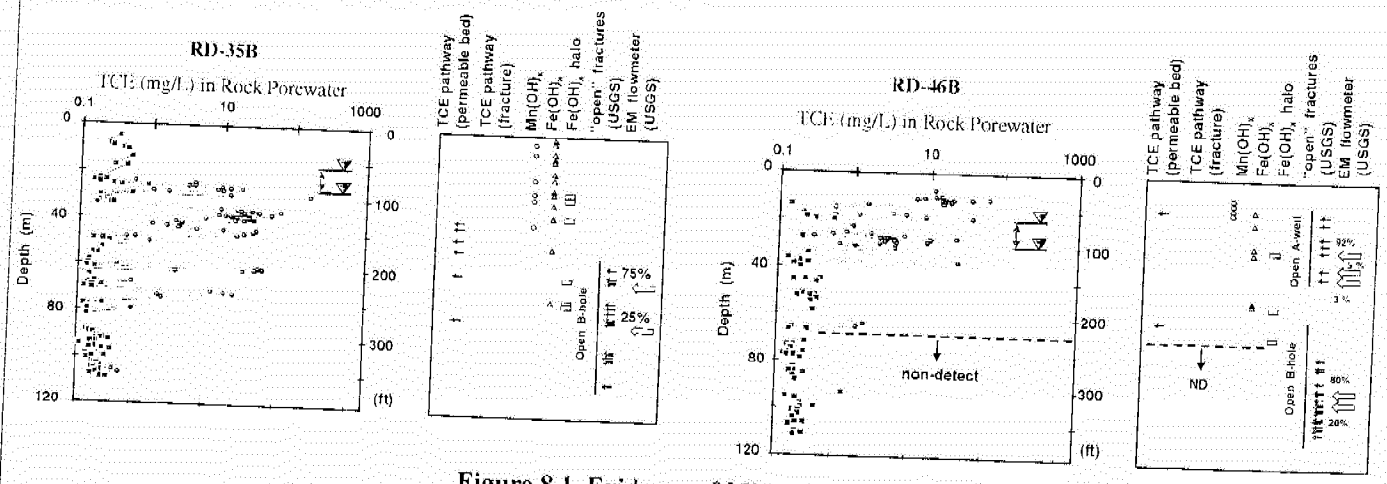

Figure 8.1 Evidence of Migration Pathways in RD-35B and RD-46B

HDMSe00012926

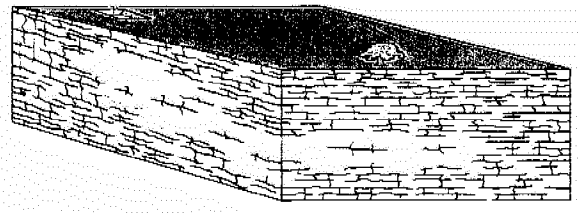

Figure 8.2 Schematic of Plume in Fractured Sandstone

This concept of a "plume" that results from the broad spatial distribution of TCE due to the interconnected fracture network and matrix diffusion was further explored using the discrete-fracture numerical model discussed in section 7.0. Additional simulations of the transport of TCE solute were performed in plan view. These simulations were performed to evaluate the pattern and extent of TCE distribution that would result in a fracture network consisting of a single plane through a "plume" in the fractured sandstone. The model domain in this simulation was 200 meters by 200 meters in the "x" and "y" directions. Other input parameters are as follows.

- uniform fracture apertures of 100 microns,
- constant source input,
- matrix porosity $\phi_m = 13\%$,
- diffusion coefficient $D_e = 1 \times 10^{-6}$ cm^2/sec,
- retardation factor associated with sorption $R_m=3$,
- hydraulic gradient, 1%
- bulk hydraulic conductivity, $K_b = 1 \times 10^{-5}$ cm/sec

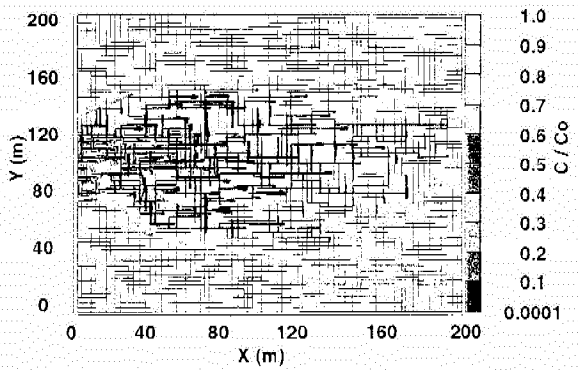

Figure 8.3 Plan View Simulation Results of Plume in Sandstone at 50 Years

The results of the modeling simulations are shown in Figure 8.3 and reveal that matrix diffusion and sorption causes the TCE solute to migrate slowly through the fracture network, thus allowing ample time to locate the downgradient extent of the plume and monitor its further migration.

The results presented in these simulations need to be considered within the context of the vertical section simulations discussed in section 7.2 (See Figure 7.8). The vertical and horizontal simulations can be considered within the context of three-dimensional space where numerous horizontal and vertical simulations represent planes or unique slices that would collectively comprise a plume. Output from the vertical simulations showing the TCE distribution in rock pore water was used to demonstrate that a monitoring device intercepting the plume would detect the TCE solute in the groundwater (Figure 8.4) These demonstrations confirm that TCE migrating through the fracture network can be located and monitored.

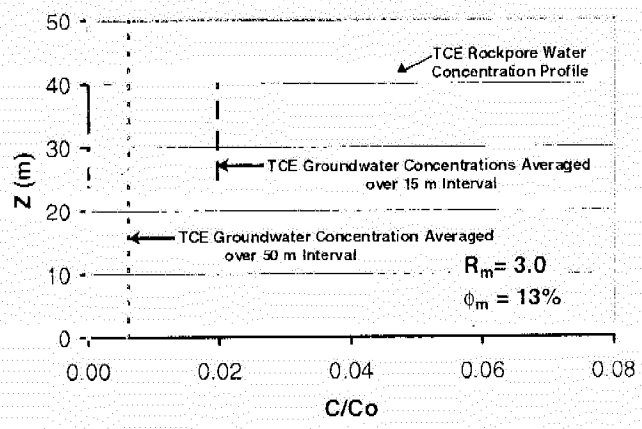

Figure 8.4 Vertical TCE Profile at X=50m after 50 years in rock porewater and in hypothetical monitoring wells with 15 and 50 m open intervals

8.3 Dispersion

Dispersion of TCE in the groundwater flowing through the fracture network has a distributory effect, i.e. the TCE becomes more broadly distributed throughout the fracture network. Dispersion is a result of molecular diffusion and

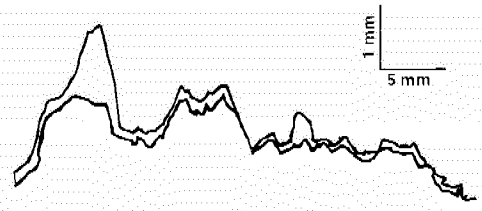

Source: NRC 1996

Figure 8.5 Variability of Fracture Aperture (Distance Between Opposing Surfaces)

HDMSe00012927

hydraulic mixing. Dispersion causes the solute concentration to decline and expand into a larger volume of groundwater than would occur only by flow (or advection). Dispersion occurs within the fracture network at two different locations: within the fracture plane and at fracture plane junctions.

Conceptually, dispersion occurs within the fracture plane due to the variability in the aperture opening (see Figure 8.5). This varying opening causes groundwater to travel on a molecular scale through different flow paths that are separated by closed contacts within the fracture plane thus creating a channeling effect. As TCE is dissolved into the groundwater flowing at different rates through the channels in the fracture plane, plume "segments" are created that have varying lateral concentration gradients as shown in Figure 8.6. The lateral concentration gradients produce dispersion within the fracture plane transverse to the direction of groundwater flow.

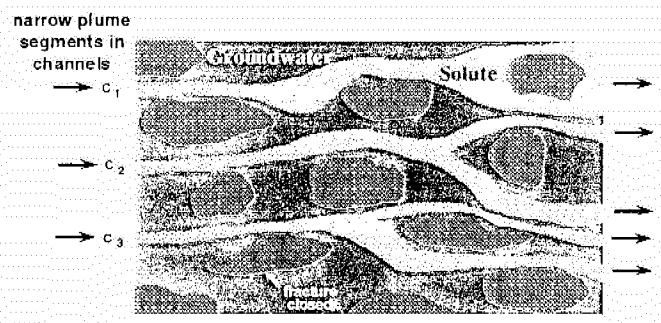

Figure 8.6 Conceptualization of Dispersion Due to Channeling in Single Fracture Plane

A field experiment was performed to evaluate the extent of dispersion within a single fracture plane at a site in Canada (Lapcevic, Novakowski and Sudicky, 1999). The experiment was initiated by injecting a tracer into groundwater flowing within the fracture plane and showed that the tracer spread both laterally and longitudinally in the mean groundwater flow direction (Figure 8.7). Transverse dispersion caused the plume to widen two to three times the source diameter and was attributed to groundwater velocity variations and closure of the fracture surfaces, which created tortuous flow paths.

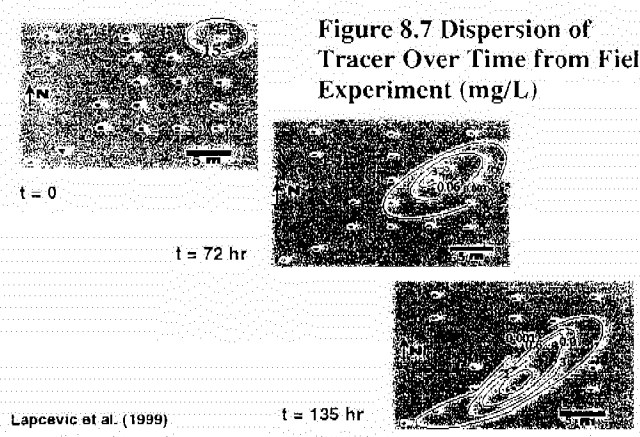

Figure 8.7 Dispersion of Tracer Over Time from Field Experiment (mg/L)

Dispersion is also expected to occur at the intersection of two fracture planes due to mixing of groundwater as shown in Figure 8.8. Laboratory experiments show that complete mixing at the intersection of fracture planes is instantaneous even under laminar flow conditions (Krizek, Karadi and Socias, 1972 and Castillo, Krizek and Karadi, 1972). Instantaneous mixing is attributed to diffusion caused by waters containing different concentrations of the solute at the intersection.

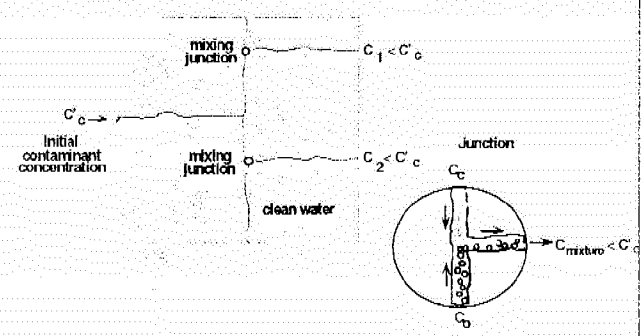

Figure 8.8 Conceptualization of Dispersion Due to Mixing at Fracture Junctions

This phenomenon causes the solute to spread orthogonal to the general direction of groundwater flow (transverse dispersion). The effects of transverse dispersion can be seen in the plan view simulations of the transport of TCE solute as shown on Figure 8.3. As TCE migrates downgradient, the width of the plume expands when compared to the plume width at the source.

The combined effects of dispersion within the fracture plane and at fracture plane junctions result in distributing TCE broadly throughout the fracture network, thereby increasing the ability to detect the plume as it migrates from the source.

8.4 Temporal and Spatial Monitoring

The effects on the transport of the TCE solute that are produced by matrix diffusion, sorption and dispersion, indicate that variations in dissolved TCE concentrations

HDMSe00012928

over time are expected to be small. This is particularly true at the SSFL where the releases occurred decades ago and the TCE migration rates likely are in the range of a few feet per year. Variations in TCE concentrations over time (years to decades) will be small (less than an order of magnitude) because of diffusion of the TCE from the matrix back into the groundwater system. Figure 8.9 and 8.10 are concentration plots over time from the numerical simulations of the transport of TCE solute that reflect the slight variations in concentrations over long time frames (100 years).

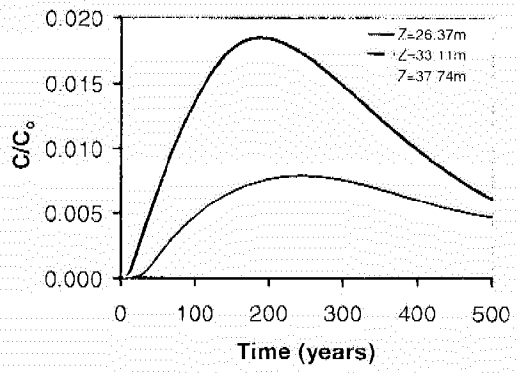

Figure 8.9 Plots of relative TCE concentrations over time in individual fractures at x=100 meters from 2-dimensional vertical modeling simulations. Note the simulations predict little variation in concentrations over a 100 year period.

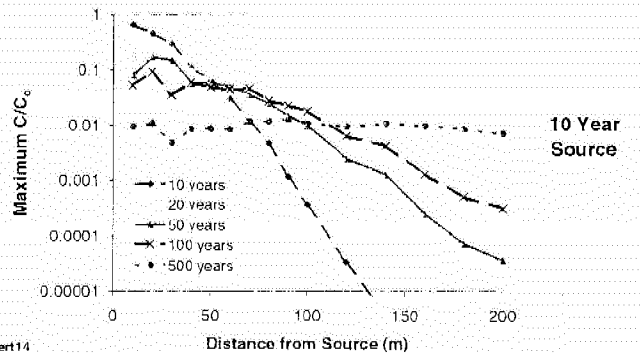

Figure 8.10 Maximum concentration over time and distance plots of TCE from single fracture modeling simulation. After 20 years, note the small variations in concentrations over long time frames at almost any distance from the source.

This understanding of the TCE migration rate indicates that periods between groundwater sampling and analysis events could be much longer than the current quarterly or even annual monitoring schedule. Variations in TCE concentrations produced by samples collected from existing monitoring wells are likely the result of several different factors that include:

- Differences in the volume of rock from which the sample was drawn based on variations in the well purge volumes between sampling events (see Figure 8.11) and,
- Changes in the groundwater flow system (e.g., changes in the groundwater extraction program) that effect the static water levels in the wells.

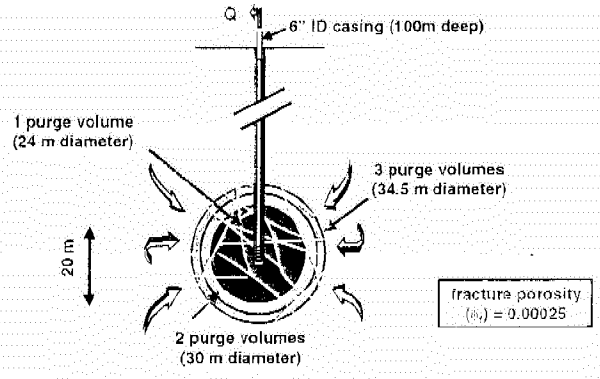

Figure 8.11 Estimated Volumes of Rock Influenced by Changes in 1 to 3 Purge Volumes

Data produced from conventional groundwater monitoring methods are difficult to interpret with regards to the spatial distribution of TCE in the groundwater. In light of the conceptual model presented in this technical memorandum, more mass is likely present in the groundwater system and sandstone matrix than can be accounted for by the dissolved concentrations in the groundwater produced by the existing monitoring well network. Efforts on groundwater characterization and monitoring in the future need to utilize new sampling and monitoring technologies which are currently available, most of which were applied at RD-35B and RD-46B.

HDMSe00012929

9.0 Summary of Conceptual Site Model

This technical memorandum has presented a conceptual model of the movement of TCE at the SSFL. The effects of the geology, hydrogeology and TCE diffusion, sorption and dispersion were considered. A summary is provided below.

1. *The fractures at the SSFL are small, systematic and interconnected.*

- Calculations of the hydraulic fracture apertures were made using site values for hydraulic conductivity and fracture spacing. Hydraulic apertures ranged from 10 to 300 microns, with a mean value of about 100 microns.
- Frequent and systematic fractures are present as evidenced by inspections of outcrops and rock core, downhole geophysics tests and the distribution of TCE in rock pore water adjacent to fractures.
- Fracture systems are interconnected as indicated by pumping test analyses, a hydraulic communication study, groundwater elevation correlations and the presence of TCE in rock pore water at numerous depths throughout the vertical profile of two test boreholes.
- Analysis of pumping test data indicated a lack of any high hydraulic conductivity zones along lineaments, suggesting that extensive open fractures do not exist.

2. *The small, systematic and interconnected fractures, coupled with the porous sandstone matrix, facilitates diffusion of TCE into the matrix.*

- Diffusion into the sandstone matrix at the SSFL has been documented by chemical analysis of 277 samples of rock core for VOCs. Samples were collected from two boreholes placed near TCE input locations. All TCE concentrations detected in rock pore water were no more than 10% of the aqueous solubility limit for TCE. These data support the conclusion that little to no DNAPL is present in fractures below the water table.

3. *TCE plume fronts are strongly retarded due to matrix diffusion and the presence of organic carbon, and advance at rates that are orders-of-magnitude slower than the average linear groundwater velocity.*

- Inspection of 15 years of groundwater chemistry data shows that TCE has not migrated far from the input locations. Maximum concentrations are also near the input locations.
- Numerical modeling simulations for TCE migration through fracture networks using properties representative of the conditions at the SSFL predict strong retardation of the TCE plume front as it migrates downgradient from the input location. The simulations also predict an overall decline in concentrations throughout the source zones and plumes.
- Inspection of the distribution of TCE in the rock core at RD-46B indicates that the plumes at the SSFL are most likely in stage 4, which is characterized by the plumes migrating very slowly and becoming stable.

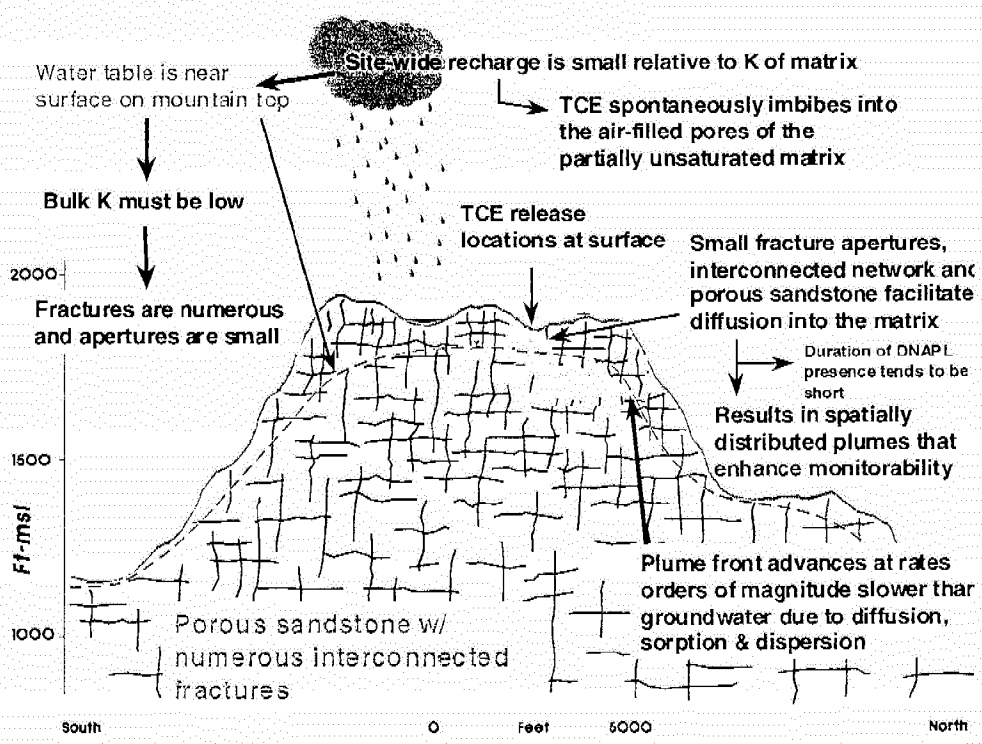

The conceptual model describing the evolution of the TCE source zone and plume, developed in this document and applied to the Chatsworth Formation at the SSFL, is supported by the mathematical modeling and field data. However, some parts of the model will require additional support. Additional field data will be acquired and mathematical modeling performed to substantiate this conceptual site model.

Figure 9.1
Graphic Depiction of Conceptual Site Model

HDMSe00012930

10.0 References

Dibblee, T. W., 1992. Geologic Map of the Calabassas Quadrangle, Los Angeles and Ventura Counties. Dibblee Geologic Foundation Map DF-37

DOE, 1989. U.S. Department of Energy, *Environmental Survey Preliminary Report*, DOE Activities at the Santa Susana Field Laboratories, Ventura County, California, February 1989

EPA, 1993. U.S. Environmental Protection Agency, *Guidance for Evaluating the Technical Impracticability of Ground-Water Restoration, Interim Final*, EPA Directive 9234.2-25, September 1993

Freeze, R. Allen and John A. Cherry, 1979. *Groundwater* (a textbook), Prentice-Hall, Englewood Cliffs, NJ 604 pp

Foster, S.S.D. 1975. The Chalk groundwater tritium anomaly-A possible explanation. Journal of Hydrology, v. 25, pp 159-165

Groundwater Resources Consultants, Inc. 1993. *Soil Sampling, Area I/Thermal Treatment Unit, June 1993*. Santa Susana Field Laboratory, Rocketdyne Division, Rockwell International Corporation, Ventura County, California, August 16, 1993.

ICF Kaiser Engineers. 1993a. *Current Conditions Report and Draft RCRA Facility Investigation Work Plan, Areas I and III*, Santa Susana Field Laboratory, Ventura County, California, October 1993.

ICF Kaiser Engineers. 1993b. *Current Conditions Report and Draft RCRA Facility Investigation Work Plan, Area II and Area I LOX plant*, Santa Susana Field Laboratory, Ventura County, California, October 1993.

ICF Kaiser Engineers. 1993c. *Current Conditions Report and Draft RCRAFacility Investigation Work Plan, Area IV*, Santa Susana Field Laboratory, Ventura County, California, October 1993.

Kirkpatrick, Glen A. 1998. Infiltration, Migration and Phase Transfer of Common DNAPLs in Naturally Fractured Clayey Aquitard: Field Experiments, M.Sc. Thesis, Department of Earth Sciences, University of Waterloo, Waterloo, Ontario, Canada

Lapcevic, P.A., K.S. Novakowski and E.A. Sudicky, 1999. The interpretation of a tracer experiment conducted in a single fracture under conditions of natural groundwater flow. Water Resources Research, Vol. 35, No. 8, pp 2301-2312.

Link, M. H., Squires, R. L, Colburn, I. P., 1981. Simi Hills Cretaceous Turbidites, Southern California. Field Trip Guide published by the Pacific Section of the Society of Economic Paleontologists and Mineralogists.

National Research Council Committee on Fracture Characterization and Fluid Flow, 1996. *Rock Fractures and Fluid Flow. Contemporary Understanding and Applications*, National Academy Press

Ogden Environmental and Energy Services Co., Inc., 1996. *RCRA Facility Investigation Workplan Addendum*, Santa Susana Field Laboratory, Ventura County, California, Volume II, Appendix C RFI Field Sampling Plans, September 1996

Ogden Environmental and Energy Services Co., Inc., 1999. *RCRA Facility Investigation, Preliminary Soil Sampling Results*, Santa Susana Field Laboratory, Ventura County, California, December 1999

O'Hara S.K., B.L. Parker, J.A. Cherry and P.R. Jorgensen, 2000. Trichloroethene DNAPL flow and mass distribution in naturally fractured clay: Evidence of aperture variability. Water Resources Research, Volume 36, Number 1, pp 135-147

Pankow, J.F. and J.A. Cherry, 1996. *Dense Chlorinated Solvents and other DNAPLs in Groundwater*, Waterloo Press, 1996

Parker, Beth L., Robert W. Gillham and John A Cherry, 1994. *Diffusive Disapperance of Immiscible Phase Liquids in Fractured Geologic Media*. Ground Water, Volume 32, Number 5, September-October 1994

Parker, Beth L, David B. McWhorter and John A Cherry, 1997. *Diffusive Loss of Non-Aqueous Phase Organic Solvents from Idealized Fractured Networks in Geologic Media*, Ground Water, Volume 35, Number 6, November-December 1997

Rocketdyne, undated. *Water Supply and Usage for Rocketdyne Propulsion Field Laboratory*, BCI 63-224 (Likely 1963)

Sage, O.G., Jr. 1971. Geology of the Eastern Portion of the "Chico" Formation, Simi Hills, California (M.A. thesis): University of California at Santa Barbara

Snow, David T., 1968. Rock fracture spacings, openings and porosities. In Proceedings of the American Society of Civil Engineers, Journal of the Soil Mechanics and Foundations Division, Volume 94:73-91

Sterling, S.N., 1999. Comparison of Discrete Depth Sampling Using Rock Core and a Removable Mulitlevel System in a TCE Contaminated Fractured Sandstone, M.Sc. Thesis, Department of Earth Sciences, University of Waterloo, Waterloo, Ontario, Canada

Sudicky, E.A. and R.G. McLaren, 1992. The Laplace Transform Galerkin Technique for large-scale simulation of mass transport in discretely fractured porous formations. Water Resources Research, 28(2): 499-514

VanderKwaak, J.E. and E.A. Sudicky, 1996. *Dissolution of non-aqueous phase liquids and aqueous-phase contaminant transport in discretely-fractured porous media*. Journal of Containmant Hydrogelogy, 23: 45-68.

HDMSe00012931